FINAL REPORT

REPORT NO. FHWA/OH-97/009

EVALUATION OF IMPROVED SHEAR KEY DESIGNS FOR MULTI-BEAM BOX GIRDER BRIDGES

Submitted to

The Ohio Department of Transportation

by

ARTHUR A. HUCKELBRIDGE, JR.
&
HASSAN HUSSEIN EL-ESNAWI

CWRU
CIVIL ENGINEERING

Department of Civil Engineering
Case School of Engineering
Case Western Reserve University
10900 Euclid Avenue
Cleveland, OH 44106

The Case School of Engineering
CASE WESTERN RESERVE UNIVERSITY
Cleveland, Ohio 44106

November, 1997

FINAL REPORT

REPORT NO. FHWA/OH-97/009

EVALUATION OF IMPROVED SHEAR KEY DESIGNS FOR MULTI-BEAM BOX GIRDER BRIDGES

Submitted to

The Ohio Department of Transportation

by

ARTHUR A. HUCKELBRIDGE, JR.

&

HASSAN HUSSEIN EL-ESNAWI

Department of Civil Engineering
Case School of Engineering
Case Western Reserve University
10900 Euclid Ave.
Cleveland, Ohio 44106

November, 1997

1. Report No.	2. Government Accession No.	3. Recipient's Catalog No.
FHWA/OH-97/009		

4. Title and Subtitle	5. Report Date
EVALUATION OF IMPROVED SHEAR KEY DESIGNS FOR MULTI-BEAM BOX GIRDER BRIDGES	August, 1997
	6. Performing Organization Code
	8. Performing Organization Report No.
7. Author(s)	
Arthur Huckelbridge	10. Work Unit No. (TRAIS)
9. Performing Organization Name and Address	11. Contract or Grant No.
Case Western Reserve University Department of Civil Engineering Cleveland, OH 44106	State Job No. 14568(0)
	13. Type of Report and Period Covered
	Final Report
12. Sponsoring Agency Name and Address	14. Sponsoring Agency Code
Ohio Department of Transportation 25 S. Front St. Columbus, OH 43215	

15. Supplementary Notes

Prepared in cooperation with the U.S. Department of Transportation, Federal Highway Administration

16. Abstract Laboratory tests were conducted to investigate the problem of shear key failure in multi-beam prestressed box girder bridges and to propose a new shear key design. Failure of shear keys will typically not only compromise the load-sharing mechanism between adjacent girders, but also may lead to the failure of the deck waterproofing system, with attendant corrosion problems.

The tests consisted of monitoring relative displacements occurring across intergirder joints, produced by a simulated concentrated wheel load. In order to economically conduct a reasonable number of tests, a 2-D "slice" of a multi-beam bridge cross section served as the basic test specimen. Finite element analyses of a three dimension bridge model showed that tensile stresses from transverse negative moments in the top flange of the bridge, generated as a result of the continuity provided by the current shear key design, may be responsible for many shear key failures.

A proposed shear key solution is presented in a new location at the neutral axis of the box girder. Finite element analysis for the new shear key location indicate an elimination of the stresses suspected of causing the failure problem. Two series of lab tests were conducted to test a two dimensional representation of the box girder bridge both under static and fatigue load. A two dimensional representative "slice" was examined by finite element analysis to define the boundary conditions required to approximate the three dimensional behavior.

A total of three lab tests were conducted for the current shear key design as well as the proposed new shear key under static loading until failure of the shear key. All tests were repeated for three different grouting materials; non-shrink grout, mag-phosphate grout and epoxy grout, except that some of the test results could be anticipated from previously completed tests.

A similar lab test program was repeated for fatigue life testing laboratory experiments. Two reaction frames were utilized, each equipped with a 50 kip (223 kN) capacity actuator and a signal generator and controller system. A computer-based data acquisition system monitored a set of DCDT's and foil strain gages during each test. Grouting materials from individual test specimens were tested for tensile strength. Load, deflection, flexural strain and fatigue life were monitored and recorded. A final series of tests was run, complete with a water-proofing membrane and asphalt concrete overlay in place, to evaluate the effect of the modified shear key design on watertightness of the longitudinal joints.

The proposed shear key, in the new neutral axis location, greatly improved the load-carrying capacity of the tested specimens when compared to the current shear key design. Utilizing a current ODOT "Type III" waterproofing membrane, at laboratory (room) temperatures in a non-chloride environment, watertightness was maintained, even in the presence of failed shear keys of the "current" design.

17. Key Words	18. Distribution Statement
	No Restrictions. This document is available to the public through the National Technical Information Service, Springfield, Virginia 22161

19. Security Classif. (of this report)	20. Security Classif. (of this page)	21. No. of Pages	22. Price
Unclassified	Unclassified		

The contents of this report reflect the views of the authors who are responsible for the facts and the accuracy of the data presented herein. The contents do not necessarily reflect the official views or policies of the Ohio Department of Transportation or the Federal Highway Administration. This report does not constitute a standard, specification or regulation.

ABSTRACT

Laboratory tests were conducted to investigate the problem of shear key failure in multi-beam prestressed box girder bridges and to propose a new shear key design. Failure of shear keys will typically not only compromise the load-sharing mechanism between adjacent girders, but also may lead to the failure of the deck waterproofing system, with attendant corrosion problems.

The tests consisted of monitoring relative displacements occurring across intergirder joints, produced by a simulated concentrated wheel load. In order to economically conduct a reasonable number of tests, a 2-D "slice" of a multi-beam bridge cross section served as the basic test specimen. Finite element analyses of a three dimension bridge model showed that tensile stresses from transverse negative moments in the top flange of the bridge, generated as a result of the continuity provided by the current shear key design, may be responsible for many shear key failures.

A proposed shear key solution is presented in a new location at the neutral axis of the box girder. Finite element analysis for the new shear key location indicate an elimination of the stresses suspected of causing the failure problem. Two series of lab tests were conducted to test a two dimensional representation of the box girder bridge both under static and fatigue load. A two dimensional representative "slice" was examined by finite element analysis to define the boundary conditions required to approximate the three dimensional behavior.

A total of three lab tests were conducted for the current shear key design as well as the proposed new shear key under static loading until failure of the shear key. All tests were repeated for three different grouting materials; non-shrink grout, mag-phosphate grout and epoxy grout, except that some of the test results could be anticipated from previously completed tests.

A similar lab test program was repeated for fatigue life testing laboratory experiments. Two reaction frames were utilized, each equipped with a 50 kip (223 kN) capacity actuator and a signal generator and controller system. A computer-based data acquisition system monitored a set of DCDT's and foil strain gages during each test. Grouting materials from individual test specimens were tested for tensile strength. Load, deflection, flexural strain and fatigue life were monitored and recorded. A final series of tests was run, complete with a water-proofing membrane and asphalt concrete overlay in place, to evaluate the effect of the modified shear key design on watertightness of the longitudinal joints.

The proposed shear key, in the new neutral axis location, greatly improved the load-carrying capacity of the tested specimens when compared to the current shear key design. Utilizing a current ODOT "Type III" waterproofing membrane, at laboratory (room) temperatures in a non-chloride environment, watertightness was maintained, even in the presence of failed shear keys of the "current" design.

ACKNOWLEDGMENTS

This research was conducted with the support of the Ohio Department of Transportation and the Federal Highway Administration. Thanks are due to Vic Dalal, Engineer, Research & Development, and the ODOT District 4 and 12 engineers. ODOT support is greatly appreciated.

Thanks are due to Robert Gulyas, Manager, Master Builders Technologies, for providing technical information about the grouting materials used in this investigation, as well as generous donations of grouting material.

Administrative staff of the Department of Civil Engineering, particularly Ms. Annette Messina, Mr. Steve Marine, Ms. Carol Dietz and Ms. Kathleen Ballou contributed mightily to this reserch effort. Their contributions are gratefully acknowledged.

TABLE OF CONTENTS

CHAPTER ONE: BACKGROUND OF THE PROBLEM

1.1 Introduction

An earlier field study [Ref. 11] of relative intergirder live load deflections in multi-beam prestressed box girder bridges indicated that the effectiveness of the shear keys currently used in this type of bridge is questionable. Failure of the shear keys, which permits greatly increased relative intergirder live load deflections, leads not only to impaired lateral load distribution, but also to degradation of the waterproofing membrane typically placed between the bridge deck and the wearing surface. Intrusion of water-born chlorides into the intergirder joints typically leads to corrosion problems, particularly of the prestressing strands adjacent to the intergirder joints. Such corrosion problems can lead to increased maintenance costs and/or shorten the useful lifetime of the bridge.

In this chapter a finite element analysis of the problem is discussed in detail. Analysis results are shown for the current design, conclusions are drawn, and a reanalysis is done for the candidate design modification. In a later chapter a series of laboratory experimental tests are presented to confirm the results obtained from the analytical work described herein.

1.2. Finite Element Analysis of Shear Keys

Finite element modeling was undertaken as a means of better understanding the behavior of grouted shear keys in multi-beam bridges and as a means of evaluating, at least on a preliminary basis, candidates for an improved design.

1.2.1. Finite Element Code

The software used to analyze the problem throughout the research was a commercial version of SAP90, a finite element package authored by E. Wilson and A. Habibullah. The version used is V5.40 [Ref 20].

The particular element used in the 3D analysis is the SOLID element. This element is for modeling three-dimensional solid structures. It is an 8-node brick element based upon an

isoparametric formulation. All stress values are calculated at the element joints in the global coordinate system.

The element used in the 2D modeling is the ASOLID element. This element is a variable 3-9 node isoparametric element which can be utilized as either a plane stress, plane strain or axisymmetric element. The element must be planar and must always exist parallel to the global principal planes The 9-node option was utilized throughout as that is the recommended formulation. Element stresses in the global coordinate system are evaluated at the integration points and extrapolated to the joints of the element.

1.2.2. 3D Model of a Box beam Subassembly

Since almost all the structure analysis software written for PC's has a limited capacity, a limitation was imposed on the problem in both the number of joints and number of elements. Nevertheless a fairly reasonable representation of a bridge box girder subassembly, consisting of three adjacent girders, was achieved.

To reduce the required three-dimensional finite element mesh to a manageable size, a 40-foot (12.192 m) long, 12-foot (3.696 m) wide subassamblage was analyzed. The bridge consists of three ODOT standard B33-48 noncomposite girders connected by the current ODOT shear key detail. By taking advantage of symmetrical conditions, the solid-element model was reduced further to represent one-fourth of the complete assemblage. The actual mesh used appears in Figure 1.1. The translations of all nodes on the X-Y plane at Z=240 inches (6099 mm) were restrained in the Z-direction (symmetric boundary condition along the midspan center line). The translations of all nodes on the Y-Z-plane at X=72 inches (1829 mm) were restrained in the X-direction (symmetric boundary condition along the longitudinal center line).

Every node was restrained against rotation about all three of the major axes. Fixed support in the Y-direction was placed along Z=0 end at the base of the box girders. The nodes from each separate girder that corresponded to a common shear-key area extending 12 inches (304.8 mm) below

the top surface of the girders, as used in the current shear key design, were given the same identity (joint number) to be constrained together for all movements. This modeling of the shear key assumes that it is capable of withstanding (without cracking) any and all stresses applied to it by the loading of any of the girders.

The length of the solid elements used was approximately 10.43 inches (265 mm) and the cross-section of the element assemblage is as shown in Figure 1.1. This model contained 2880 joints and 1656 elements. Material properties were introduced to the program in the form of a modulus of elasticity for concrete =3600 ksi (24822 MPa) and Poisson ratio of 0.15.

The analysis took place for a concentrated "wheel" load equal to 10 kips (44.5 kN) on the centerline of the midspan section. This load was calculated so as to equal to one double wheel load of the AASHTO, [Ref. 2], standard HS20 truck shown in Figure 1.2. The static load shown is 32 Kips / 4 = 8.0 Kips (35.58 kN). An average impact factor was estimated from equation 1.1. contained in the AASHTO standard specifications, Article 3.8.2, to be approximately 25% for spans ranging from 40 to 100 ft (12.192 to 30.48 m).

This load was used throughout the study and will be referred to as the standard wheel load. Please note that for the purpose of the study and the comparison between different alternatives, the analysis will be done for a single wheel load, since the nearest possible adjacent wheel load will not be closer than 4 ft (1.22 m), and nearly all of the lateral distribution from a wheel load was found to take place within approximately one foot (.3048 m) longitudinally in either direction from the actual load point.

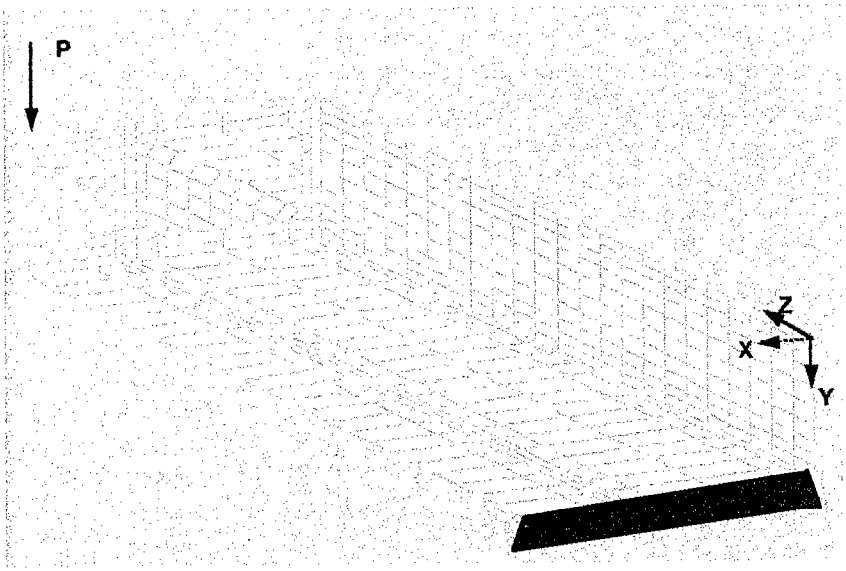

Figure 1.1 3-D Finite Element Mesh of 3 Girder Subassemblage

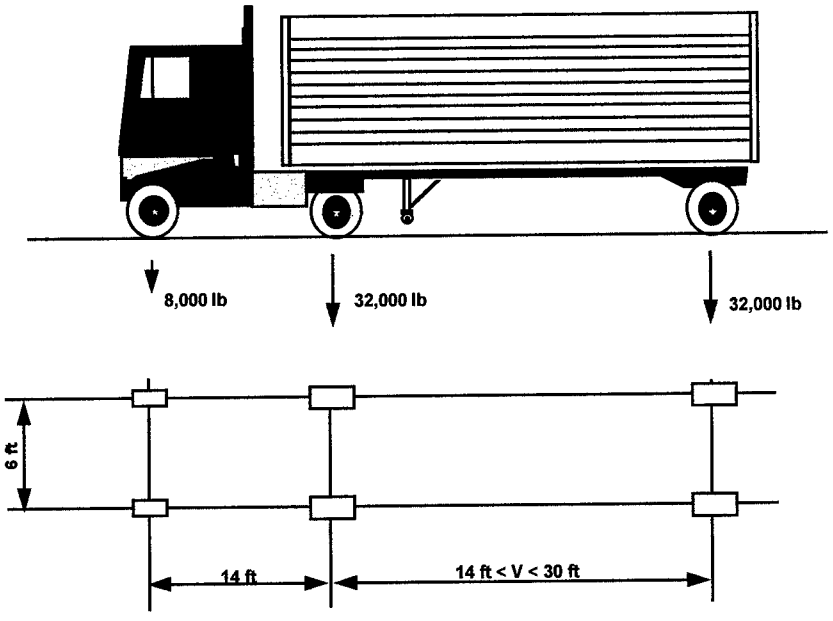

Figure 1.2 Standard HS20 Truck

Figure 1.3. illustrates the distribution of maximum principal stresses, σ_1, for the midspan cross section of the 3D mesh. Since this current ODOT shear key is grouted flush to the top surface of the top flange, it creates significant transverse flexural continuity between the top flanges of adjacent beams. Significant transverse (negative moment) tensile bending stresses are thus introduced in the top of the shear region. Looking closer to the shear key at the top outside surface, a value of approximately 60 psi (414 kPa) transverse tensile stresses can be reached due to this single wheel loading. It is reasonable to envision that tensile stresses of such a magnitude, applied many times over the course of several years of service loading, could lead to longitudinal cracking and a progressive failure of the grouted shear key.

It is also very possible that the occasional overload, either due to a specially permitted or illegal vehicle, could lead to an instantaneous failure of the shear key, as could excessive shrinkage or temperature stresses.

Figure 1.4. illustrates also the deformed shape of the midspan cross section under loading. This figure, accompanied with the previously shown stress contour figure, describe a presumed cause of failure for the current design of the shear key. It is almost certainly not a "shear" failure, as might be anticipated from the function of these keys. The apparent initiation of any load-induced crack is more likely due to the "negative" transverse bending stress, attributable to the lateral frame action due to the continuity at these regions provided by the grouted shear key.

Failure of a shear key due to tensile stresses can be occur in one of two forms, either failure of the grouting material itself due to low tensile strength, or due to failure of the bond between the grouting material and the concrete section. For most grout materials, it is to be expected that a bond failure will precede failure of the grout or the adjacent concrete.

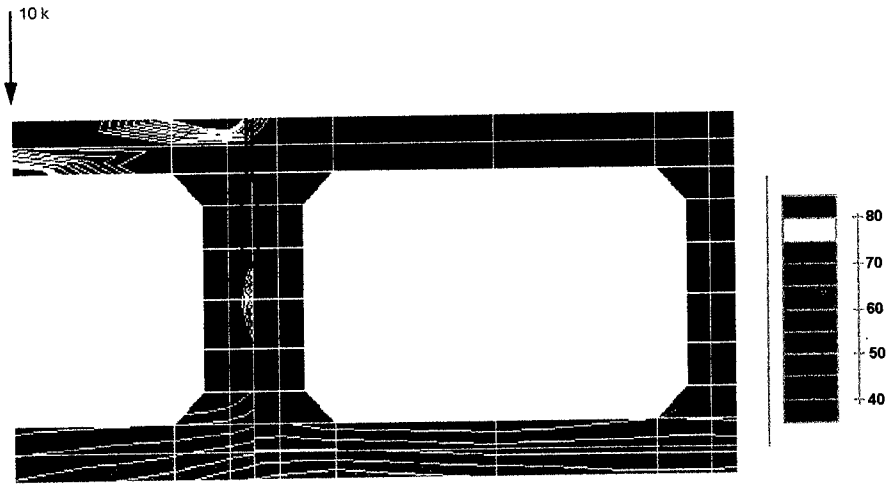

Figure 1.3 : Principal (σ_1) Stresses (psi) @ Midspan Cross Section;
Current Shear Key Design

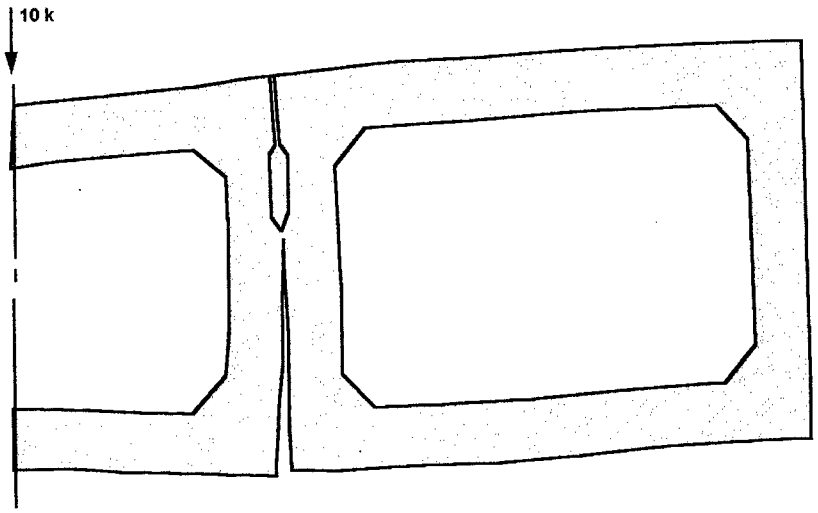

Figure 1.4: Deformed Shape of Midspan Cross Section of 3 Girder Subassemblage

To solve this problem, one can think in one of the following options; either to find a different grouting material which can resist this kind of repeated tensile stress, or to reduce the tensile stresses at this region or to eliminate completely this kind of stress by changing the design. These options will be briefly referred to here.

1.3.1. Grouting Materials

In this study, three different grouting materials were tested as a component material of a structural "shear key" in the composite assemblies. These grouting materials are frequently used in DOT work.

1.3.1.a. "Non-shrink" Grout

Non-shrink" Grout is the conventionally used grout in key-ways. It is a non-shrink cement, easy to prepare and can be mixed to a flowable degree, which eases the grouting process. Its normal setting time gives a convenient time window to mix, transport and place it but does possibly present delays to use of heavy equipment in overlay placement. The compressive strength of this type of grout is between 5000 to 6000 psi (34475 to 41370 kPa). In general it must meet the required minimum properties as specified in ASTM C 1107 [Ref. 1].

1.3.1.b. Magnesium Ammonium Phosphate [Mg-NH_4-PO_4] Mortar

The commercial brand used in this study is "SET-45 Grout", manufactured by Masterbuilders, Inc. The retarded version of this product was used as it has greater fluidity, and has lower heat generation than the regular formulation, which is typically used in rapid repair of bridge decks and pavements. This product had been used on several precast prestressed bridge projects in the northwest and Alaska. It was also approved by DOT in the US and Canada.

1.3.1.c. Filled Epoxy Resin Mortar

Filled epoxy resin mortar is used by number of bridge engineers as a shear-key grouting material. This use of filled epoxy grout is relatively new, but is growing. Epoxy resin is a good adhesive for most materials used in construction. It greatly enhances the adhesion of the grout to

concrete surfaces. Also, it possesses increased strength and exhibits reduced permeability of the grout mix.

In contrary to the relationship between steel and concrete, epoxy has a major difference from concrete in its coefficient of thermal expansion. This difference is potentially a considerable problem which requires careful consideration. The thermal coefficient of epoxy-aggregate systems will be reduced as the aggregate content of the system is increased, as indicated in Figure 1.5. [Ref. 3]. However the expansion coefficient of the epoxy is considerably higher than concrete . The higher elastic modulus of concrete tends to restrain the movement of the epoxy, thereby causing potentially severe thermal stresses at the interface. These stresses will first affect the weaker material, which will be the concrete side, and initiate cracks in it at the interface region.

A finite element analysis was conducted to study the effect of temperature rise on an epoxy grouted shear key in a concrete box girder. Figure 1.6. shows the mesh utilized for the analysis, symmetric geometry and loading condition were taken advantage of. Boundary conditions were applied to allow free expansion in both longitudinal and transverse directions. Thermal coefficients were considered 6E-06 in/in/°F (1E-05 cm/cm/°C) for concrete and 18E-06 in/in/°F (3.2E-05 cm/cm/°C) for epoxy grout, as obtained from Figure 1.5. The modulus of elasticity was assumed to be 2000 ksi (13.8 GPa) for epoxy grout and 4000 ksi (27.6 GPa) for concrete. A temperature rise of 40° F (22° C) was applied to the structure. Figures 1.7. and 1.8. shows the longitudinal and principal stresses computed from the finite element analysis.

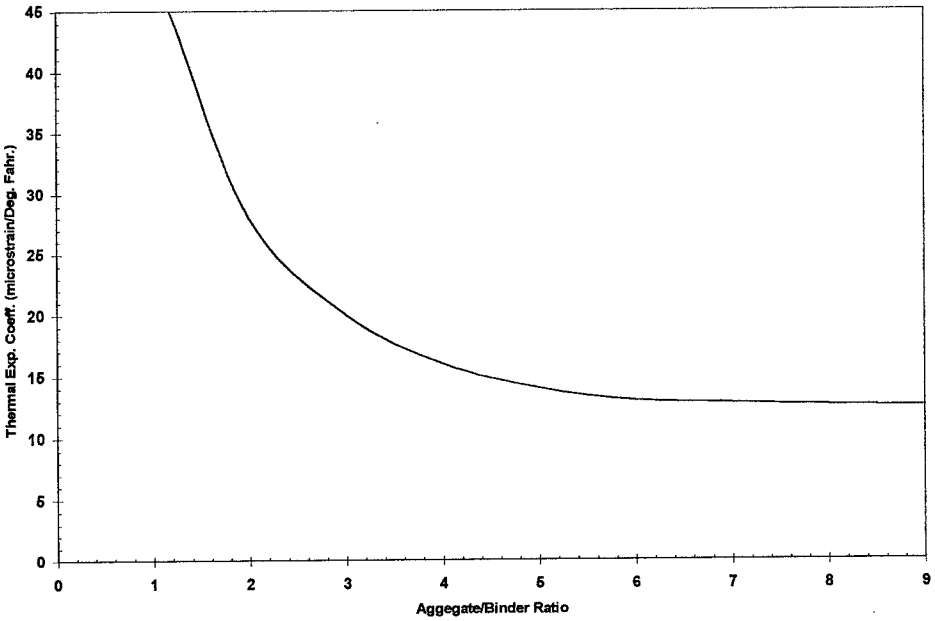

Figure 1.5 Effect of Aggregate/Binder Ratio on the Themal Expansion of Epoxy Grout

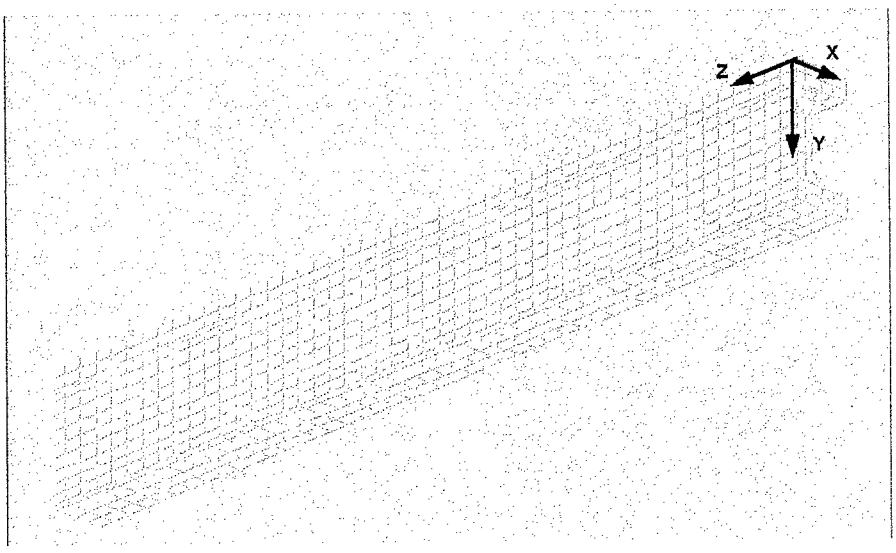

Figure 1.6: FE Mesh for Thermal Stress Analysis with Epoxy Shear Key

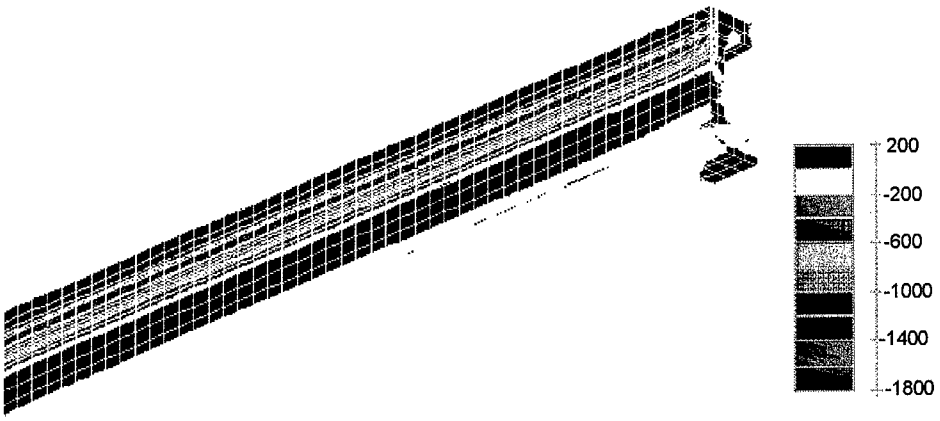

Figure 1.7: Longitudinal Sresses (psi) Due to a 40 deg. F Temperature Change with an Epoxy Shear Key

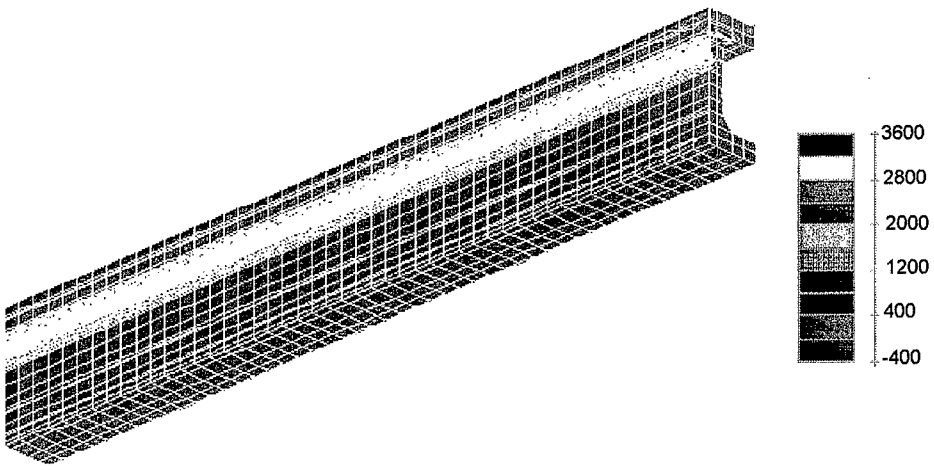

Figure 1.8: 1st (σ_1) Principal Stresses (psi) Due to a 40 deg. F Temperature Change with an Epoxy Shear Key

Results indicate a low tensile stresses in the major part of the concrete cross section and a high compression stresses in the shear key part of the structure. Both materials can presumably tolerate these kinds of stresses. The non reinforced concrete portion of the section adjacent to the shear key, however, is exposed to high stresses due to the restrained conditions provided by the adhesion between the two materials, combined with the differences in the expansions implied by the 12E-06 in/in/°F (2.1E-05 cm/cm/°C) difference in the thermal coefficient. Knowing that these stresses are additional to the service stresses, one can readily believe that there is cause for concern with major temperature changes, when using epoxy grout in concrete structures.

1.3.2. Transverse Post-tensioning

Another suggestion toward solving this problem was, simply, to introduce transverse compression prestress at the shear key region. The idea is to offset the tensile stresses along the transverse section created by the continuity made with the current shear key location. The only readily apparent possibility to accomplish this result is by the introduction of compressive prestress force into the keys through transverse post-tensioning of the assembled girders. Figure 1.9. illustrates the distribution of transverse stresses, produced by transverse post-tensioning forces of 40 kips (177.9 kN) , applied on 12 ft. (3.66 m) intervals to the flanges of the same three girder assembly model shown earlier in section 1.2. The level of prestress was selected to represent the maximum force achievable with a single 7 wire strand; the spacing was selected to be compatible with the practice of utilizing one standard tie rod for spans up to 25 feet (7.6 m) .

It appears from this analysis, that to be fully effective, transverse post-tensioning with conventional 7 wire strands would require such close strand spacing (perhaps on the order of 2.5 ft (.76 m)), that much of the economic attractiveness of the box girder structural system would be sacrificed. More equipment, materials, labor, time, supervision and quality control would be

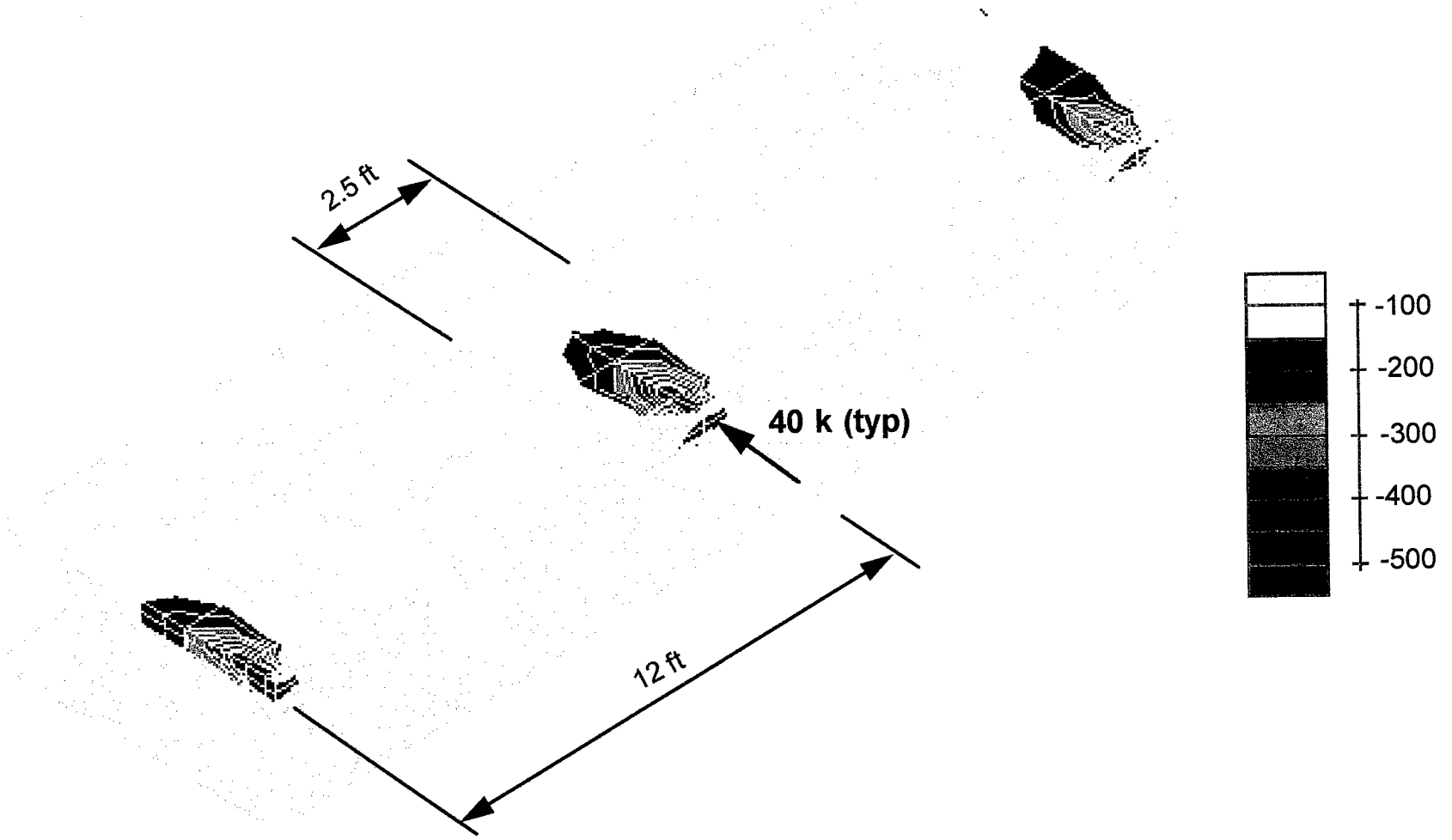

Figure 1.9: Transverse Stresses (psi) Due to Post-tensioning @ 12 ft Intervals

required; however, there is no reason to assume transverse post-tensioning would not function well structurally. It will not, however, be considered further as a candidate solution in this study.

1.3.3. Redesign of the Shear Key

By looking closely at the stress distribution in Figure 1.3., one can imagine that the way to eliminate this kind of tensile stress, is to remove the continuity element, the shear key, from this location. Since the basic structural use of these shear keys is to transfer shear forces from one girder to another, a new location can be chosen any where along the side of the girder, where it contacts the adjacent girder. The location which can transfer shear forces should not be so far from the top that it can not be easily grouted, yet far enough from the top flange level so it does not create continuity between adjacent flanges. Structurally the optimum location is near the neutral axis of the section. In this study the term redesign or new design will be limited to choosing this new location.

A similar finite element model to the one mentioned in 1.2. was used to investigate the effect of a relocated shear key. A set of nodes near the mid-height of the girders were joined to represent the new candidate location of the shear key. This set of nodes extends approximately 3 inches (76.2 mm) above and below the horizontal centerline of the section.

Figure 1.10 shows the transverse stress distribution at midspan for the analysis of this subassemblage. Flexural continuity is now broken between the adjacent top flanges, and only minimal tensile stresses exist in the shear key region, on the order of 20 psi (138 kPa). These tensile stresses are primarily due to longitudinal bending moments in the girders, and should not lead to longitudinal cracking and subsequent failure of the shear key. Figure 1.11. shows also the deformed shape of this solution which shows considerably less lateral frame action than with the original shear key configuration.

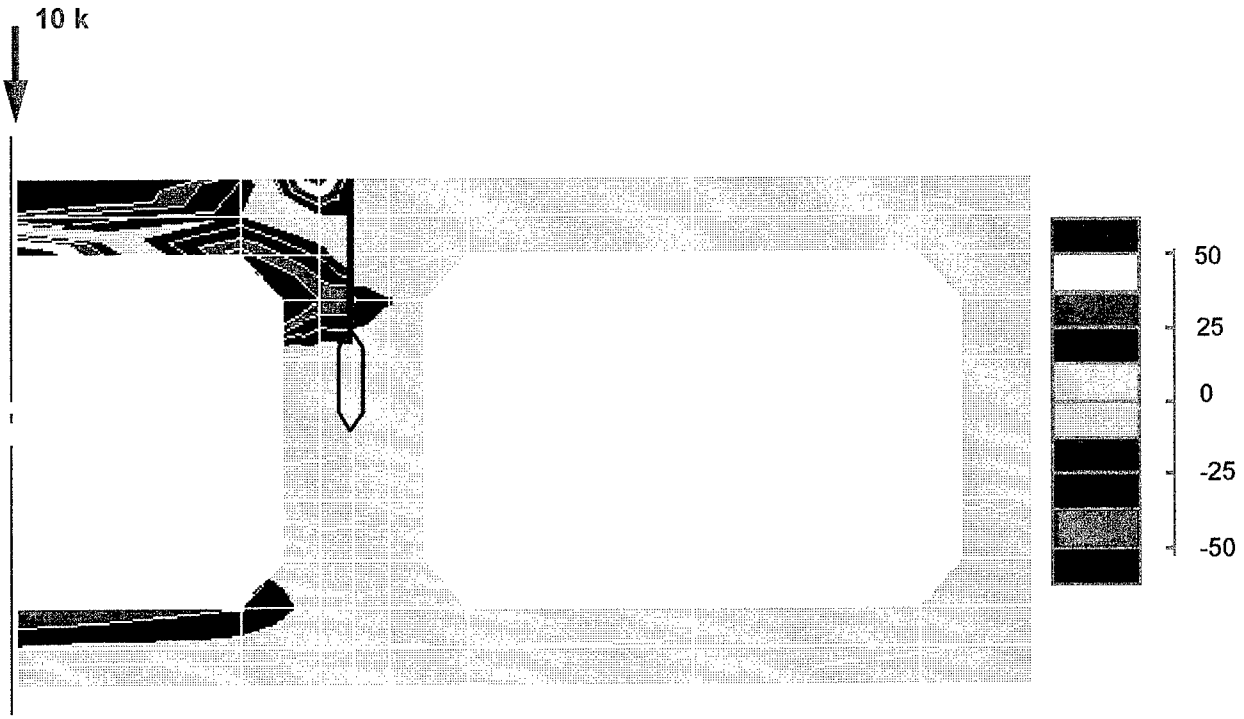

Figure 1.10: Transverse Stresses (psi) @ Midspan for the Modified Shear Key Design

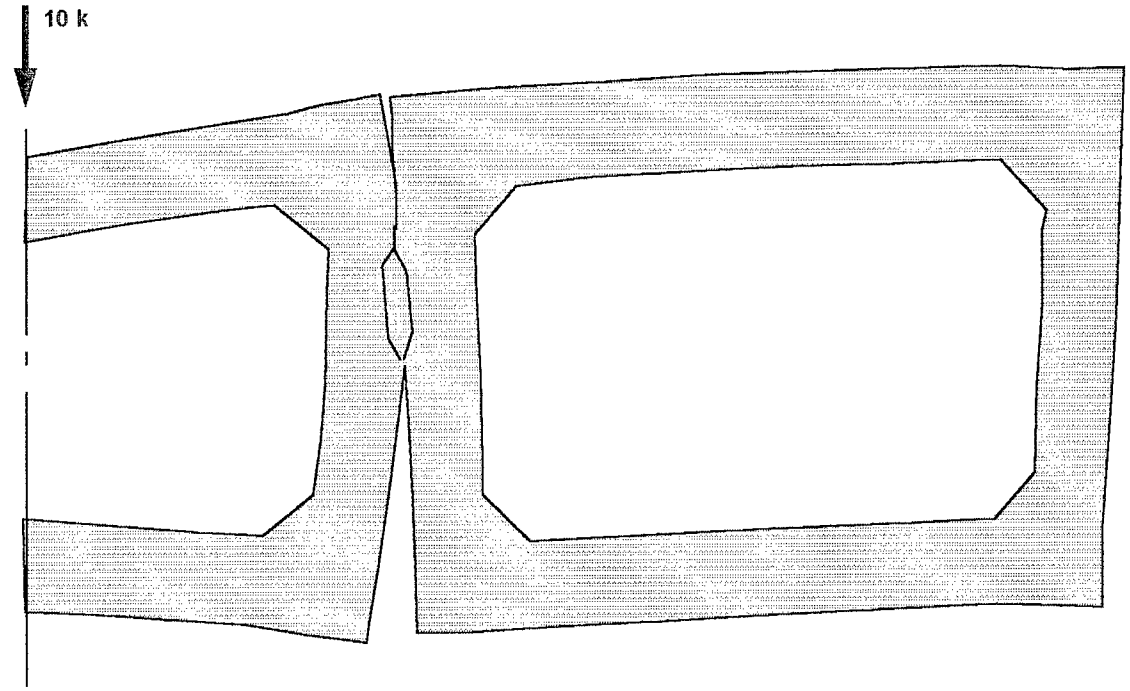

Figure 1.11: Deformed Shape; Midspan X-Section & Modified Shear Key Location

CHAPTER TWO: EXPERIMENTAL PROGRAM

2.1. Introduction

In this chapter an experimental program is presented to verify the effectiveness of the third solution suggested in the previous chapter. This verification is carried out through a comparison of the results for a shear key located in the current position, at the top flange, and a shear key located at the neutral axis, the suggested candidate design. Both sets of tests will be done for the different grouting materials referred to in chapter one.

Since scaling down the shear key, with its small width of 1.5 inch (38.1 mm) would lead to a scale model shear key with dimensions less than typical construction tolerances allowed in concrete members, a full scale test is desirable. On the other hand, it is difficult to accommodate a three dimensional, full scale laboratory model with a minimum span of 40 feet (12.19 m). Therefore a two dimensional model was utilized to test shear keys, representing a slice of the bridge at midspan, with a full-scale cross section, as illustrated in Figure 2.1. Elastic supports, which simulated the actual in-service support conditions for such a girder "slice", were provided.

2.2. Two dimensional representation

Before planning the laboratory test program, a planar finite element analysis was performed for the proposed test assembly, to compare the predicted 2-D to the 3D analysis, discussed and shown earlier. By this comparison process, the desired stiffness in the supports in order to simulate the actual 3D behavior could be quantified. Figure 2.2. shows the finite element mesh used to analyze a three girder subassembly. After analyzing a number of trials, the best simulation of 3-D behavior was identified as the test setup shown in Figure 2.3. The quasi-rigid supports at the two ends of the two exterior girders, with the center girder supported totally by the shear keys, provided a similar stress distribution and deformed shape to that observed in the 3-D analysis.

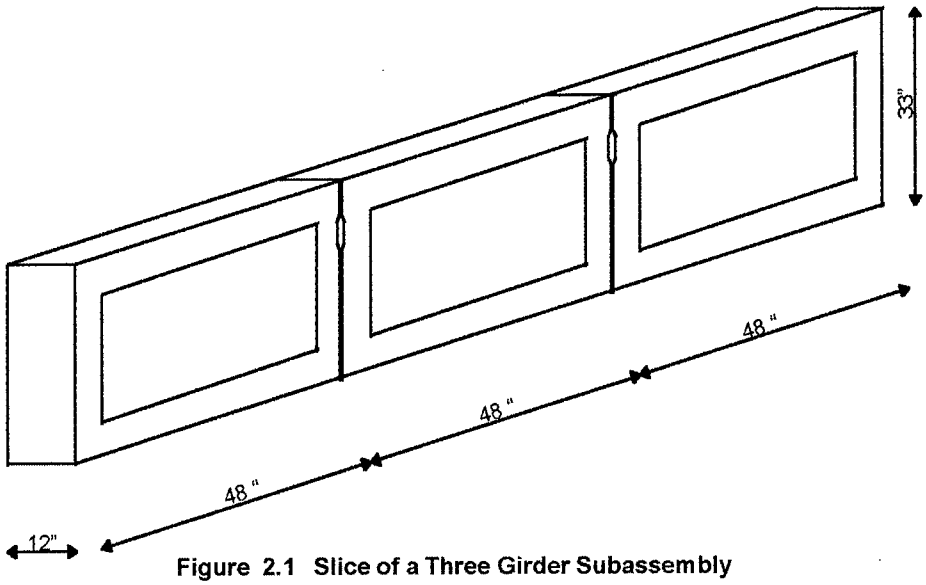

Figure 2.1 Slice of a Three Girder Subassembly

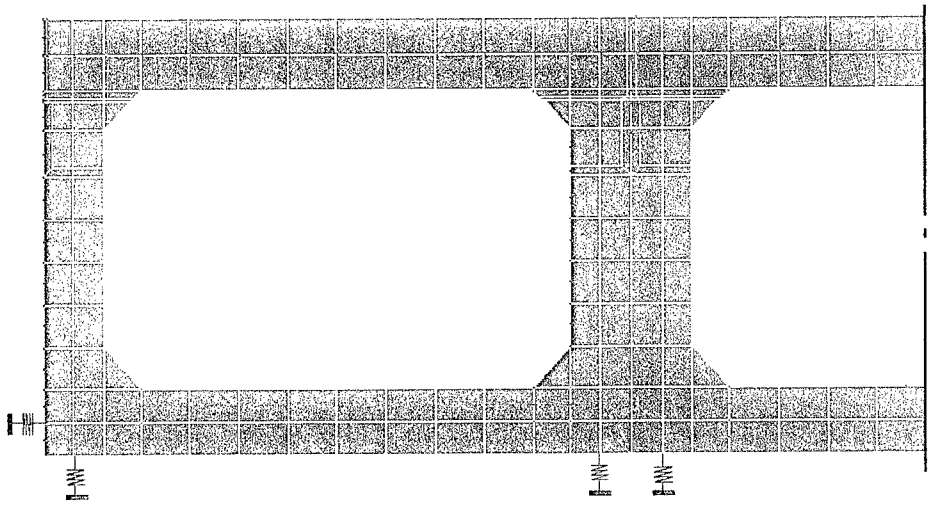

Figure 2.2 : Plane Stress Finite Element Mesh for 2D Analysis

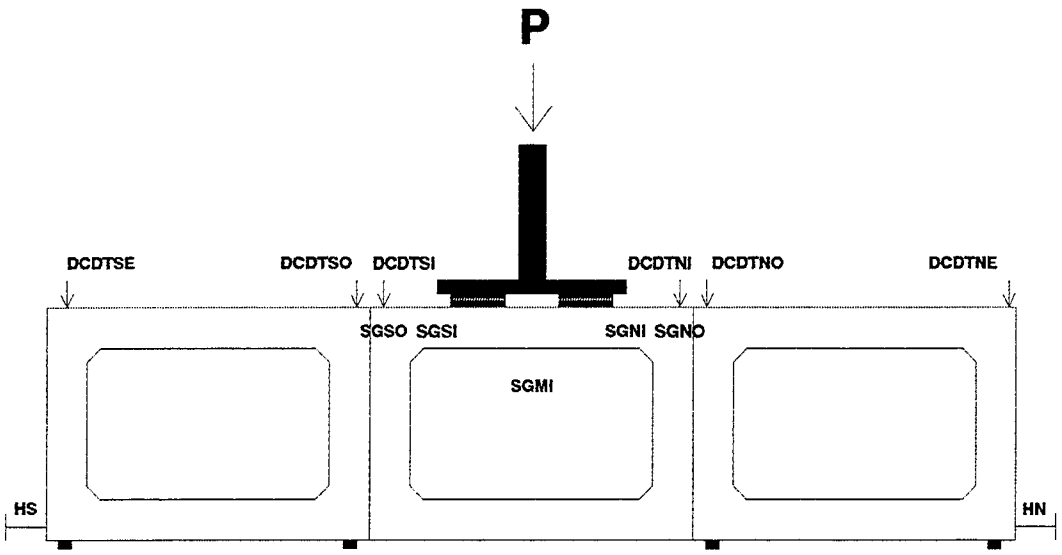

Figure 2.3 General Assembly for a Planer 3 Girder Test

The horizontal elastic support at the exterior sections simulate the torsional rigidity of a box girder for the corresponding spans. The described boundary conditions give compatible finite element results between the 2-D and 3-D cases, with respect to deformation and stresses, both in distribution and magnitudes. Figure 2.4. and Figure 2.5. show both deformed shape and stress distribution for the three girder assembly with the current top key used and single concentrated load of 10 kips (44.5 kN). Two factors affected the choice of the "slice" thickness; the space available, within the reaction frame used for loading the specimen, and the capability to handle and move the individual components. A slice thickness of 12 inches, for a full scale cross section, was chosen as a practical dimension to work with; it was also noted that most lateral load transfer through such shear keys takes place within one foot of a concentrated load application point.

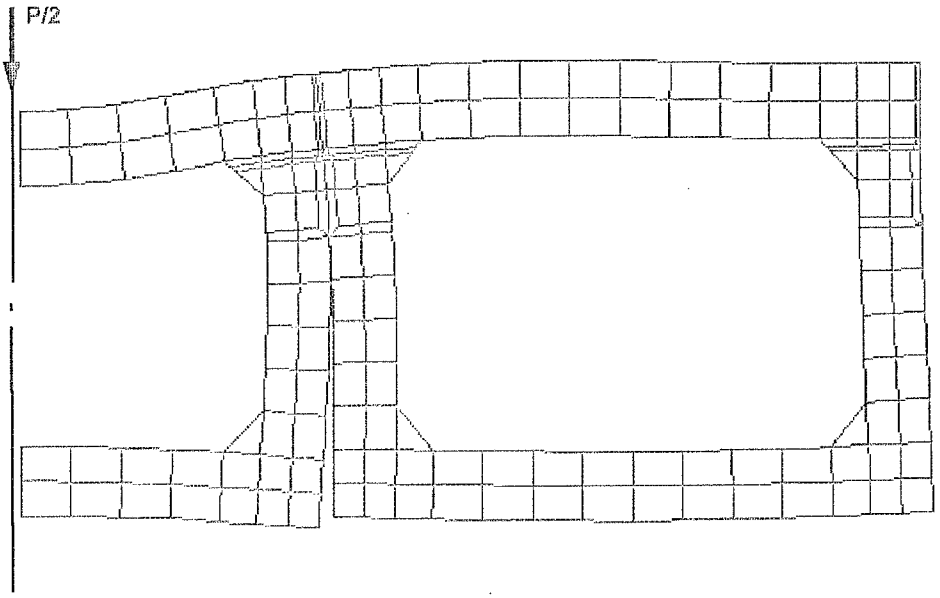

Figure 2.4 : Deformed Shape for 2D FE Mesh;
3 Girder Subassembly "Slice" Specimen

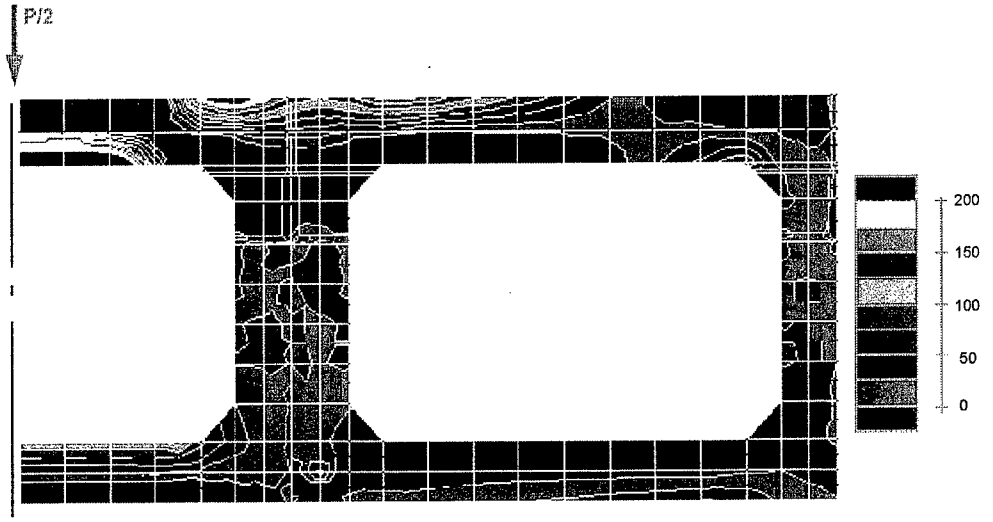

Figure 2.5: Principal (σ_1) Stresses (psi) Due to 10 kip Wheel Load;
2D (12 in. Thick) Slice FE Mesh

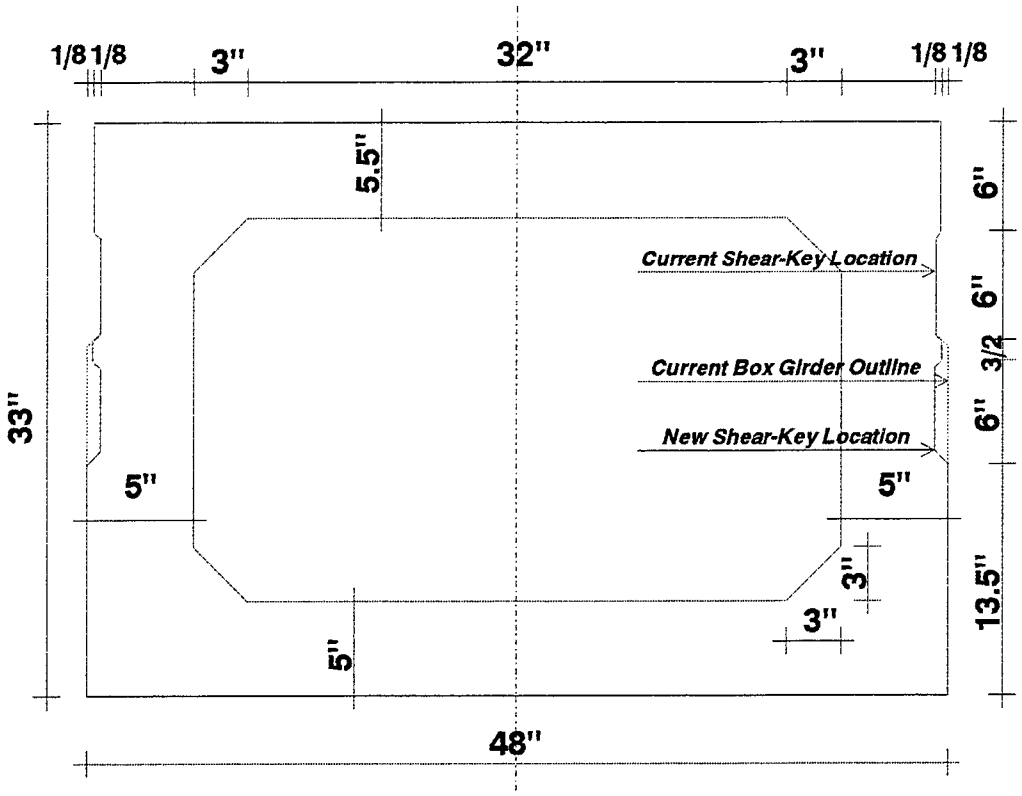

Figure 2.6. Cross-section Dimensions of the Test Specimens

2.3. Test Specimen

Detailed dimensions for the section used are given in Figure 2.6. The top recesses form the keyway in its current location. The lower recesses form the keyway for the suggested new location. The same section was used both for the test of the current as well as the suggested shear key, in order to minimize the number of concrete sections needed for the research program.

Concrete forms were fabricated "in house", with a "negative" key way form, made of teflon, to provide a concrete surface finish similar to that produced by the steel forms used for real bridge girders.

The concrete used was commercial ready-mix with a minimum specified compressive strength of 5000 psi (34475 kPa) and 6% air entrainment. Standard cylinders were taken, cured under

the same conditions as the specimens, and tested after 28 days. The measured average compressive strength was 6000 psi (41.37 MPa).

Since these tests were for a 2D transverse slice, longitudinal prestressing wires were not provided. Short pieces of #3 bars were used to hold the reinforcement cage together. Since the investigation was to be directed at the shear key and not the beam cross section, an increase of the typical transverse reinforcement was utilized to increase the capacity. This strengthening helped ensure the survival of the cross sections through multiple test sequences. The top flange has one additional transverse #4 bar compared to what would be utilized in a field girder flange. All reinforcement used were grade 60 No. 4 bars, except for the No. 3 ties. Figure 2.7. shows the reinforcement details used for these sections. Figure 2.8. shows the forms used with the "negative form" attached to it. Figure 2.9. shows the reinforcement cage, and finally Figure 2.10. shows the placement of concrete and finishing operations.

After pouring the concrete in the forms mechanical vibration was used to compact the fresh concrete and expel air bubbles. The exposed concrete surface was finished and cured under wet burlap for 24 hours. Form sides were removed at 48 hours and the curing process continued for another week. Sections were then stored until the time of actual testing.

2.4. Test Setup

The experimental testing was performed in the Structural Laboratory of the Civil Engineering Department at Case Western Reserve University. This laboratory contains a structural component testing area, 14 ft (4.27 m) x 60 ft (18.29 m) in plan, with tie-downs capability on a 2 ft (0.61 m) square grid. The testing floor is the 18-in. (0.46 m) thick top flange of a 12-ft. (3.66 m) deep reinforced concrete box girder. An in-house machine shop was utilized to fabricate the concrete specimen forms and perform all other tasks for fixture fabrication and maintenance.

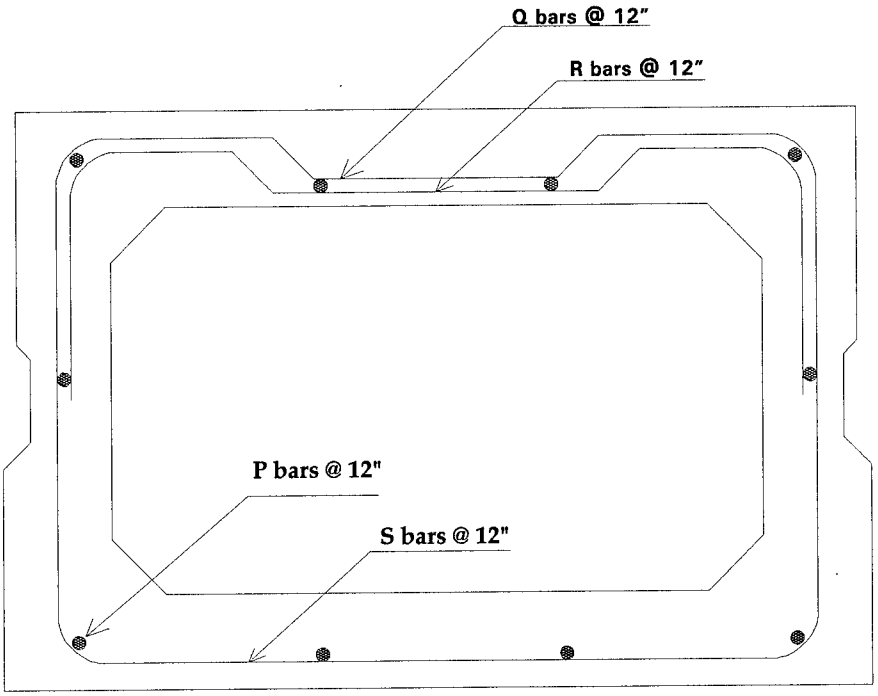

Figure 2.7. Typical Reinforcement For Sec B33-48

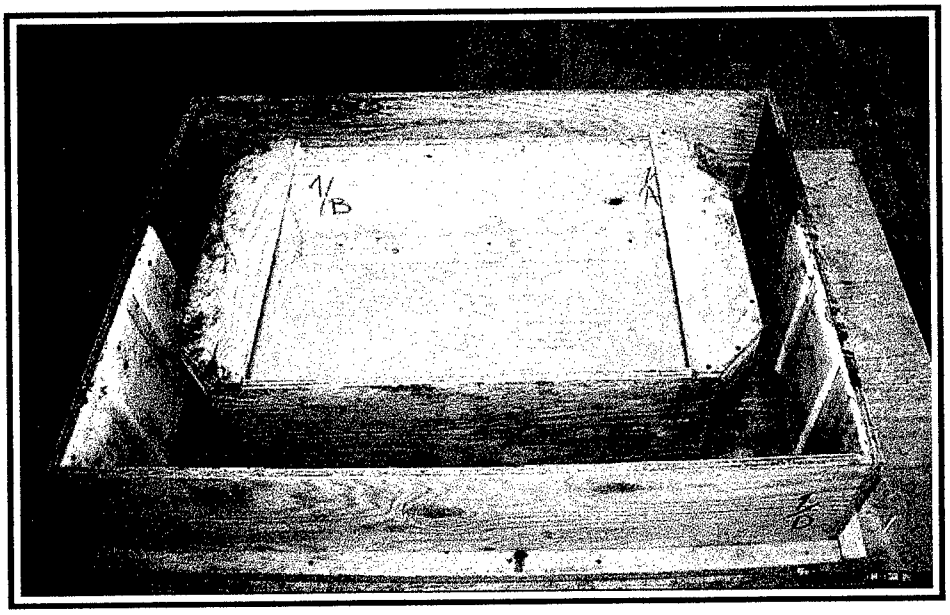

Figure 2.8 Assembled Form with Keyway Blockout

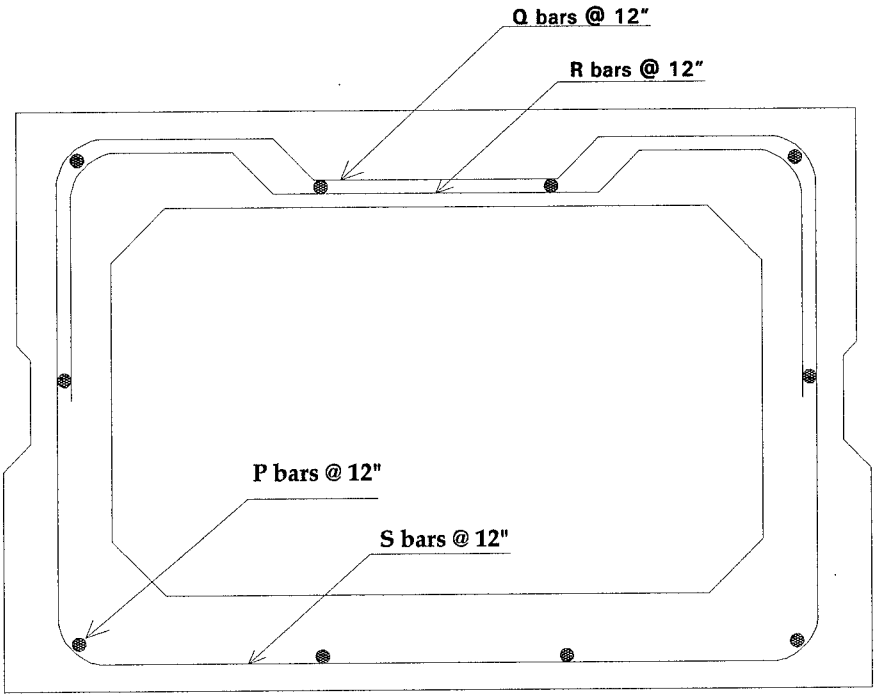

Figure 2.7. Typical Reinforcement For Sec B33-48

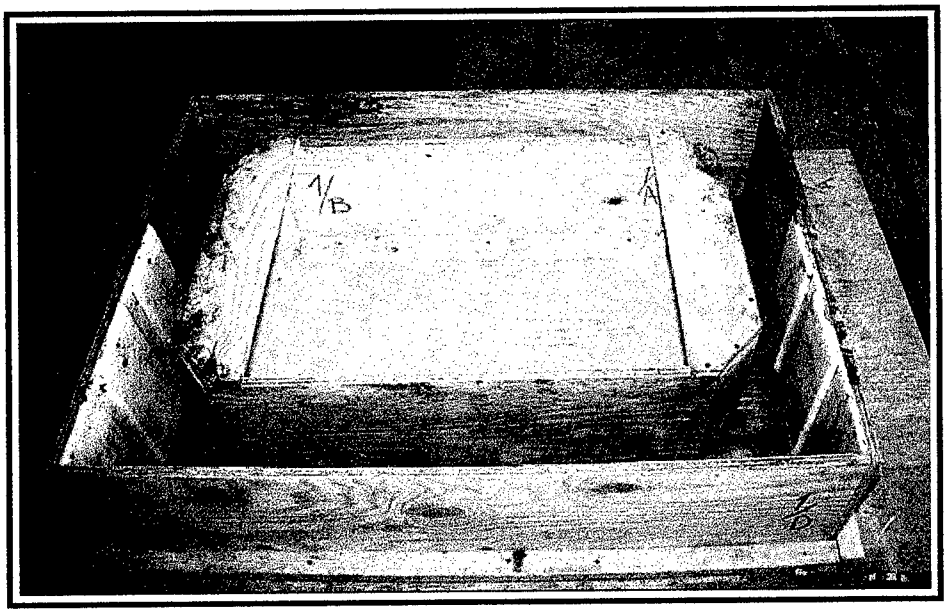

Figure 2.8 Assembled Form with Keyway Blockout

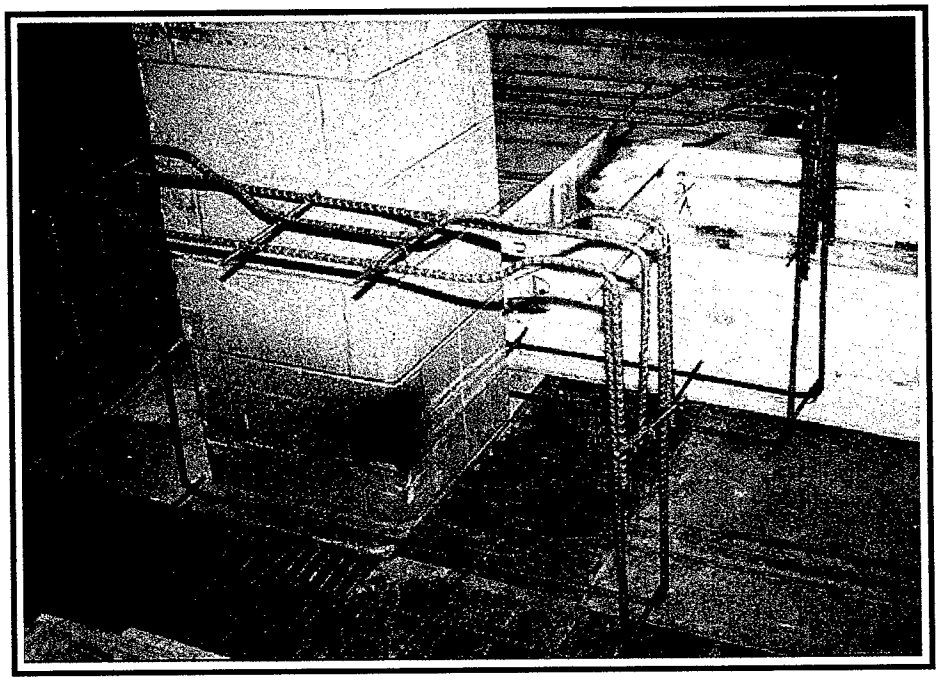

Figure 2.9 Reinforcement Cage Used for Test Specimen

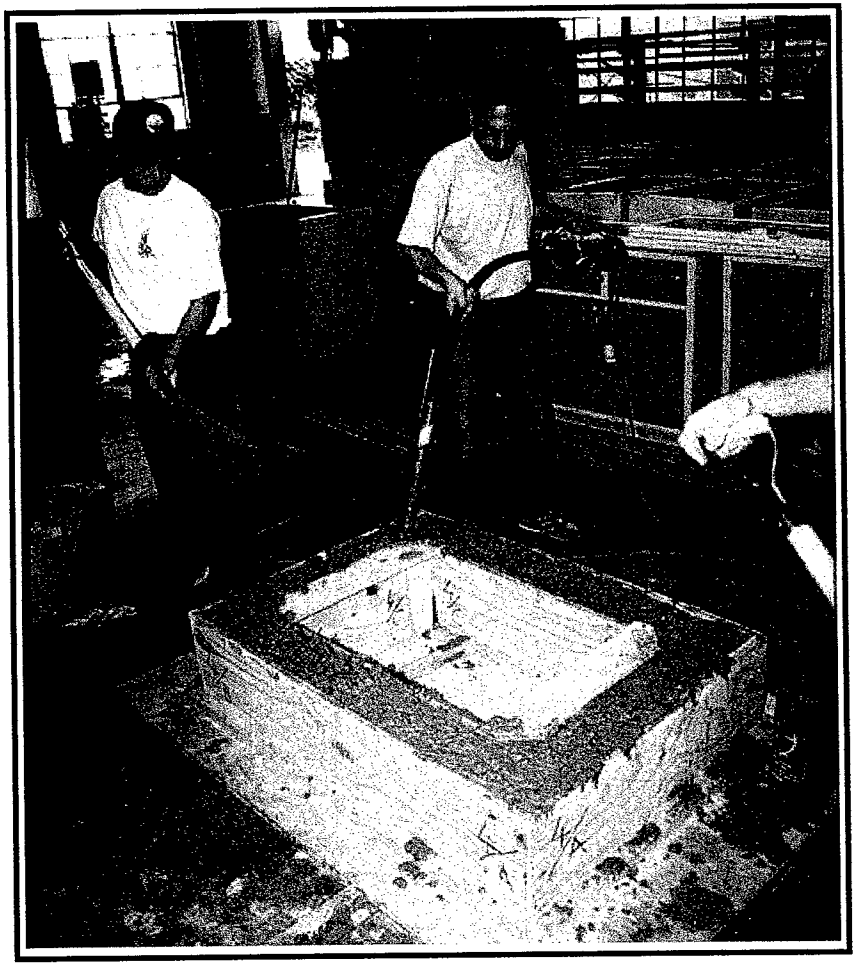

Figure 2.10: Placing and Vibrating Concrete

2.4.1. Loading

The loading fixture utilized for the static and cyclic load tests was a steel reaction frame bolted to the laboratory structural floor, and an MTS servo-hydraulic actuator with a load capacity of 50 kip (223 kN) and a maximum stroke of 6 in. (152.4 mm). The simulated concentrated wheel-load was applied to the top flange of the specimen at specific locations through a steel plate attached to the actuator. For the static load test, the loading rate was approximately 150 lb/sec (667.2 N/sec). The cyclic load tests were performed using load control, at a frequency of about 3 Hz. The cyclic load varied sinusoidally, with a minimum load level of about 500 lb (2.224 kN), to ensure stability of the test specimen, and a maximum load level equal to 10,500 lb (46.8 kN).

According to the AASHTO specifications, article 3.30 [Ref. 2], the tire contact area should be assumed as a rectangle with an area in square inches of 0.01P, and a length in Direction of Traffic/Width of Tire ratio of 1/2.5, in which P = wheel load in lb. For this research P was calculated to be 8,000 lb (35584 N), see article 3.2., This makes the contact area required equal to 80 in^2 (51612.8 mm^2). To represent a dual tire footprint, two combined wood and rubber blocks of 4 in. (101.6 mm) width and 10 in. (254 mm) length were used to apply the load to the top flange. The blocks were centered on the concrete surface as shown in Figure 2.11. The magnitude of the applied load is monitored by means of the internal load cell of the actuator.

2.4.2. Displacement measurements

A set of direct-current-displacement-transducers (DCDT's) were used to measure the vertical displacement of the girder's end corners, and the corners adjacent to the shear keys. These measurements quantify the shear keys displacement response to the loading, as well as help identify the shear key's failure. Also these measurements give an idea about the global structural behavior under the given boundary conditions, to be compared with the 2-D or the 3-D analysis, and the field

tests. The DCDT's used had a range of ±0.5 in. (±12.7 mm); they were calibrated before running each test, using an input excitation of 6 volts.

2.4.3. Strain measurements

To obtain strain measurements in the concrete cross sections, three foil-backed strain gages were used at each monitored section. The Epoxy-bonded electrical resistance strain gages were located at the maximum expected tensile stress locations on the top flange of the loaded cross

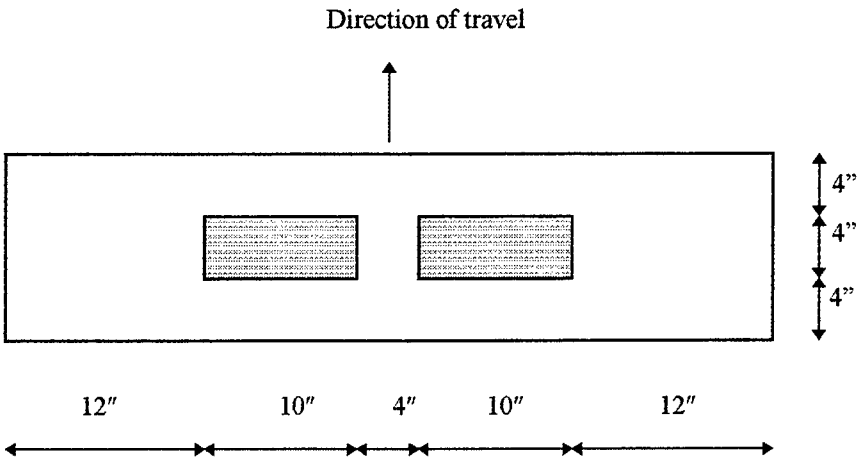

Plan View of the Simulated Tire Footprint

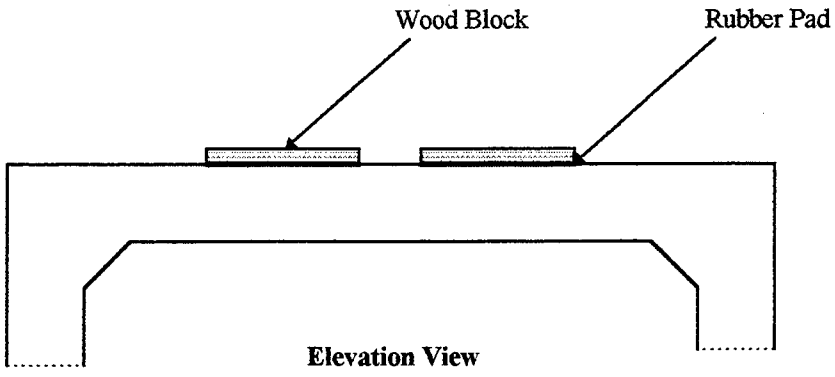

Elevation View

Figure 2.11. Arrangement and Dimensions of Load Contact Blocks

sections; Figure 2.3. shows the locations of the strain gages. The strain gages used were of a type designated EA-06-10CBE-120, manufactured by Measurements Group, Inc.

2.4.4. Data Acquisition

The data acquisition in this study was performed by a system that included a PC, a Keithley-500A Data Acquisition System and the Lab Tech Notebook software package.

2.5. Test procedures

Table 2.1. shows the matrix of planned tests for the course of this study. Later, at certain points of the testing process, some of the tests were determined to be unnecessary, as a consequence of early test results.

The plan, as pointed to earlier, was to test the 2D specimens in two phases. the first phase was the static test series, referred to with (S), carried out monotonically until failure of the shear key. The objective of this test is to determine the static capacity of the shear key, and obtain the corresponding factor of safety against the design loads. The second phase was the stationary cyclic loading (D) with a standard design load amplitude. The objective of this test was to clarify the effect of the fatigue on the shear keys. Both phases included tests for the top key (TK) which is the current location of the shear key as well as the middle key (MK) which is the suggested new location of the shear key. All tests were planned to be repeated at least three times (1,2,3), for all three types of grouting materials, Non-shrink set grout (A), Set-45 grout (B) and Epoxy grout (C).

Test Labels / Test Type		Grouting Material		
		Non-Shrink Grout	Mag-phosphate Grout	Epoxy Grout
Phase I Static test	Top Key	TKSA1,2,3	TKSB1,2,3	TKSC1,2,3
	Middle Key	MKSA1,2,3	MKSB1,2,3	MKSC1,2,3
Phase II Pulsating test	Top Key	TKDA1,2,3	TKDB1,2,3	TKDC1,2,3
	Middle Key	MKDA1,2,3	MKDB1,2,3	MKD1,2,3

Table 2.1. Experimental test plan

2.5.1. Static tests

The surfaces of the concrete sections which form the key way for the shear keys were prepared just prior to assembling the specimen and grouting the shear keys. Several different surface preparation procedures were tested. Preparing the surface is important to create a surface suitable for achieving bond with the grouting materials, and expose any trapped voids near the surface. It is also important to clean the surface from any carbonated concrete. A power grinder was used for surface preparation, as well as a power wire brush during the testing program. For shear keys grouted with mag-phosphate grout, a portable sand-blaster was used to better simulate field surface preparation techniques. One set of sections was taken to an actual construction site and commercially sand blasted; results of these preparation techniques will be discussed later in this study.

A typical specimen assembly procedure went as follows: three sections were placed together, touching each other at the sides, and the faces were aligned. The two exterior sections were supported by 2x12x1 inch (50.8x304.8x25.4 mm) steel plates, one under each web. The middle section was supported with temporary shims to level it with the other two sections, until grouting. Lateral inclined braces were erected at the ends of the top flange of the section and secured to the structural floor to ensure out of plane stability during testing. The open sides of the shear keys were closed by forms clamped to the concrete sections. The bottom of the shear key was blocked with foam. When epoxy grout was used, plastic envelopes were used for the wooden side forms to ease form release.

Producer's instructions were followed when mixing the grouting materials. Non-shrink grout was moist cured directly after grouting at the top surface, and later when forms were released the next day, at all exposed surfaces. Curing typically took place for seven days, or until sufficient strength was deeloped, prior to testing. No particular curing process was required, for the mag-phosphate grout nor for the epoxy grout.

During grouting of shear keys, test specimens of the grout were cast for quality control. Typically six briquet "dog bone" grout specimens were tested for direct tensile strength according to the ASTM standard C 307, specifications [1]. Also, six 2x4 in. cylinders were prepared for both splitting tensile strength and compressive strength tests, to satisfy the ASTM standards C 496-90 , C 109-92 and C 93-90. Figures 2.12., 2.13 and 2.14. show the material test specimen and testing machines.

Table 2.2. shows the averaged results of the grouting materials quality control tests. It is worth mentioning that the direct tensile strength tests for the epoxy mortar were not possible to obtain, due to difficulties in removing the specimens from the molds.

TEST RESULT ⇒	**Grouting Material**		
TEST TYPE ⇓	**Non-Shrink Grout** **psi**	**Mag-phosphate Grout** **psi**	**Epoxy Grout** **psi**
Compressive strength	5500	5000	13000
Direct tensile strength	495	425	N/A
Splitting tensile strength	505	445	1725

Table 2.2. Grouting Material Properties

Prior to testing, horizontal restraints, mentioned in article 2.2., were wedged at the bottom of the exterior sections sides. These elastic supports were reacted by a steel beam bolted to the test floor. These horizontal supports were instrumented to provide a horizontal reaction time history during tests. DCDT's were mounted on a reference beam bolted to the structure floor, running parallel to and at the height of the test specimen. The DCDT's, strain gages, as well as the load cell, were all connected to the data acquisition system. Adjustment of the zero reading for

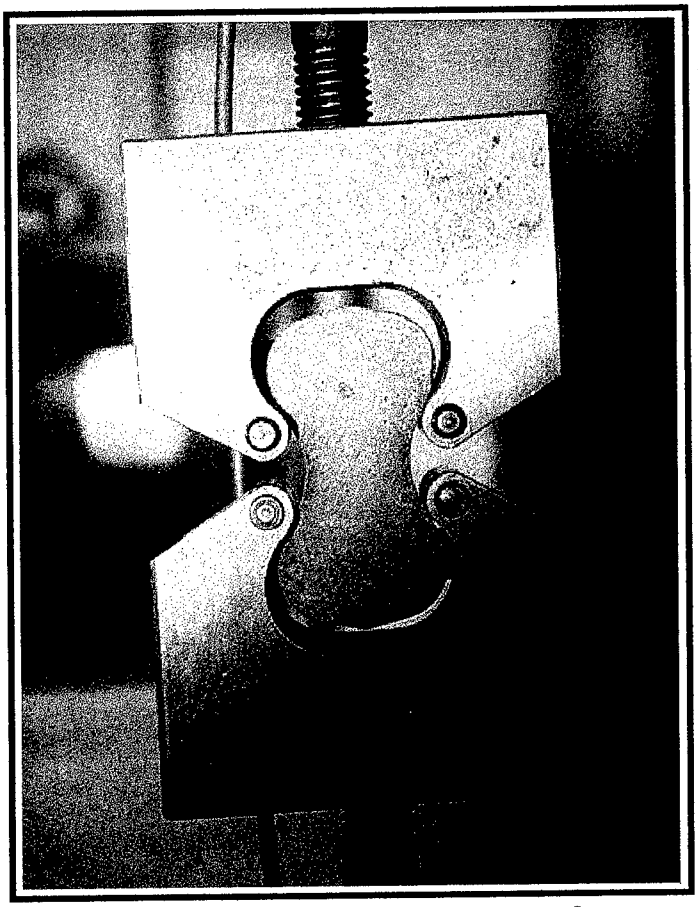

Figure 2.12 Direct Tensile Tests of Grout Coupons

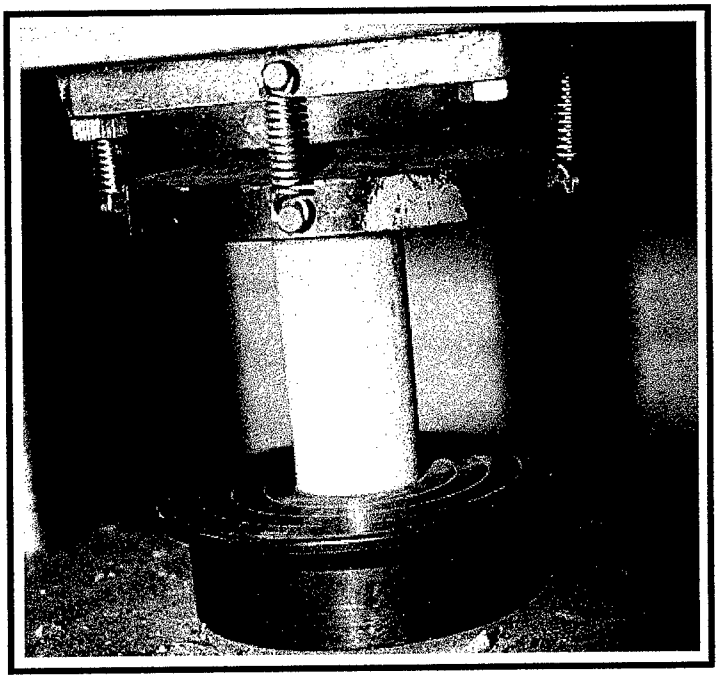

Figure 2.13 Standard Compression Test of Grout Cylinder

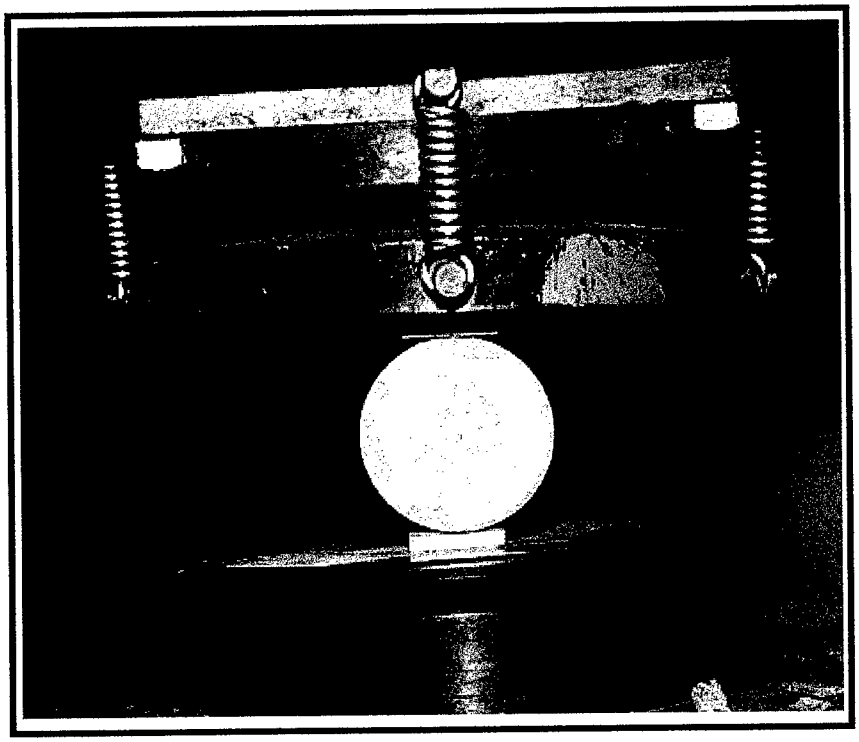

Figure 2.14: Standard Splitting Tensile Strength Test of Grout Cylinder

the strain gages and the DCDT's was carried out after setting up the software for the number of channels and the data file formats. Temporary supports of the middle section were removed prior to initiation of testing. After starting the data acquisition system, loading was started while monitoring the behavior of the concrete section, the data display and most importantly the shear key cracking. Figure 2.15. illustrates the assembled test specimen with the grouted shear keys and all instruments attached, ready to proceed with a test.

2.5.2. Fatigue tests

2.5.2.1. Single point loading

Using a stationary cycling load, the fatigue tests were carried using a similar setup to that utilized for the static load tests. Instead of loading the test specimen to failure, however, loading was cycling between load levels 0.5 kip and 10.5 kips, as described in 2.2. The number of cycles until cracking was recorded. Tests were conducted for all different grouting materials.

4.5.2.2. Out of Phase Loading

In addition to the single point loading fatigue tests, utilizing three beam sections, a four girder assemblage was tested under an out-of-phase loading, as shown in Figure 2.16. The two middle sections, connected with a center shear key, are loaded in a sinusoidal fashion with a 180° phase lag between the two loads which simulates the shear reversals applied to a center joint on a 2 lane highway. Experience from field tests indicate that this load condition, when present, is particularly demanding for grouted shear keys.

Supporting condition for a four section assemblage differed from the three section one, since the test configuration did not contain the same load symmetry as the previous case. A number of trials were simulated on a finite element model representing this test to determine the best representative support condition. The best simulation resulted from rigid supports at the outside ends of the exterior sections, (indicated numbers 1 and 8 in Figure 2.16.), and elastic supports at all other section ends,

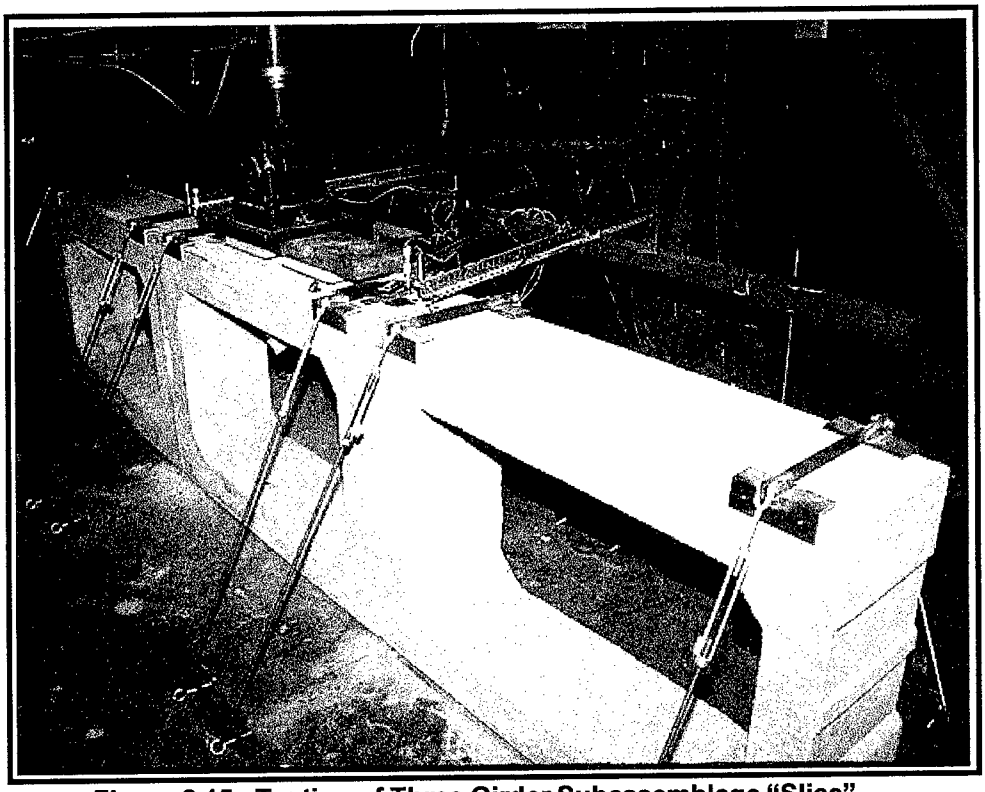

Figure 2.15: Testing of Three Girder Subassemblage "Slice"

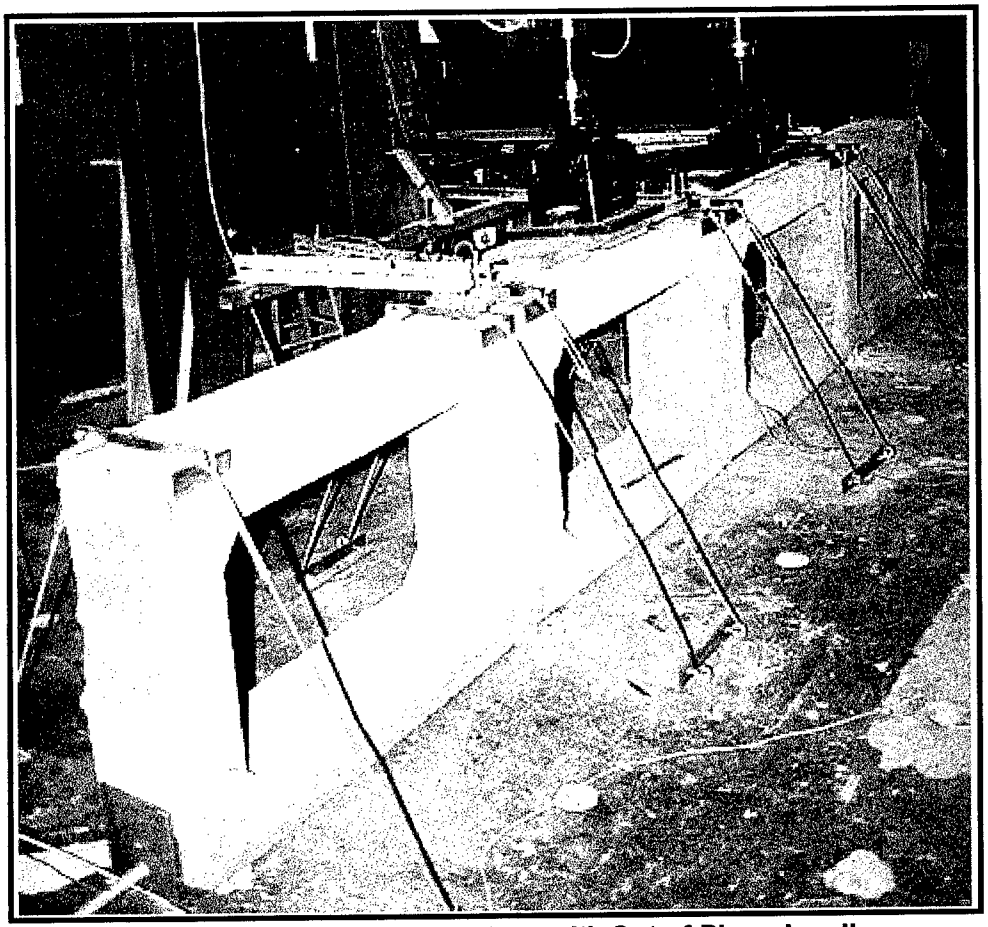

Figure 2.17: 4 Girder Subassemblage with Out-of-Phase Loading

(indicated numbers 2,3,4,5,6 and 7 in Figure 2.16.). An elastic coefficient of 600 kip/in. (105.1 kN/mm) obtained by using a combined steel and rubber supports, was determined to best simulate observed stress distributions. Also, horizontal elastic supports were utilized as in the previous setup. Figure 2.17. shows a typical test setup for the 4 girder, out-of-phase, load test.

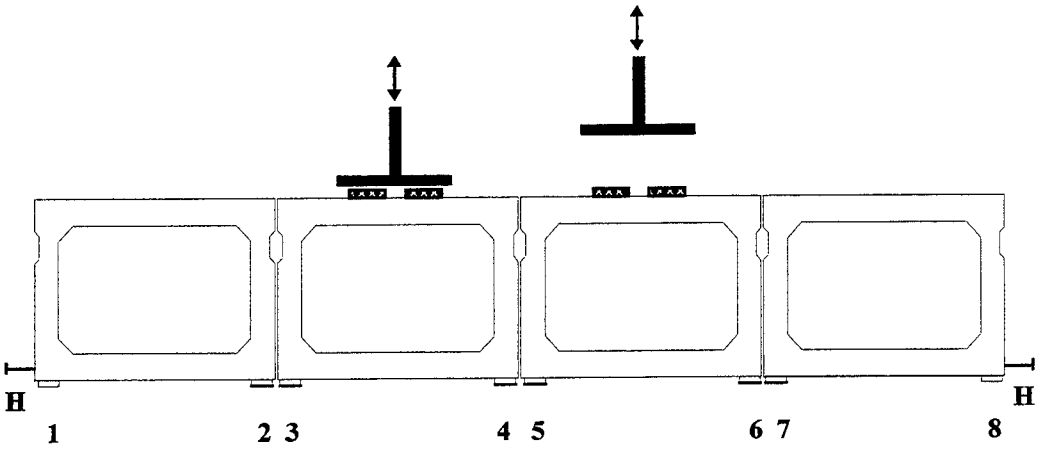

Figure 2.16. Fatigue Test Under Out-of-Phase Loading

Setup procedures were the same as the three girder static load tests. To start the loading cycling for both the three girders and the four girders assemblages, the load set point were established at half the design load plus the offset. The frequency was maintained at 3 Hz for specimen stability. The load range was increased gradually to reach the desired peak/valley values. The number of cycles were recorded for each test. Strain and displacement were monitored intermittently for selected tests.

CHAPTER THREE: RESULTS AND DISCUSSION

3.1. Introduction

The results in this chapter will be presented separately for both test types, static and fatigue tests. Comparisons will be presented for both groups between the cases of the current shear key design, and the modified shear key design for every tested grouting material. Some of the planned tests listed previously in the experimental program were not completed since those results could be logically predicted from the previously completed tests in the program. On the other hand, at the end of this chapter, results of two additional tests which were not listed in the planned experimental program will be presented.

The principle indicator of failure of the shear key is the visual observation of a crack initiating at a particular static load value or load cycle number. In all cases, once a crack is initiated it does not take much additional load or many more repeated cycles to propagate it and cause shear key failure. The observed values of static load or load cycle number at which the crack first initiated were recorded. The expression "failure" in this study is meant to indicate a crack propagated through the grouted material of the shear key, or more often a debonding between the grouted shear key and the concrete surfaces.

In addition to the visual observation of the crack initiation, an analysis of the collected data, in the form of displacements as well as the strain measurements, was utilized to help identify shear key failure. Strain gages immediately adjacent to the keyway interface (and perpendicular to it) on the top flange would typically give an indication of a drop in tensile stress upon initiation of a crack at that interface (which was the failure mode of essentially all the specimens utilizing the current keyway design). Strain gages on the "inner" surface of the top flange, near the midspan region (directly below the load application), would also typically give an indication of a an increase in tensile stress at failure of the keyway, due to the the loss of of continuity across the keyway region; this indicator was sometimes masked, however, by initial flexural cracking of the top flange midspan

region itself. In addition, independent measurements of vertical and horizontal displacements on each side of the shear key would typically give an indication of keyway failure.

3.2. Static Test Results

3.2.1. Non-shrink Grout Shear Key Tests

This material was a major consideration in this study since conventional non-shrink grout is the cheapest and most commonly used type of grouting material. Most of the field observed problems were in bridges with shear keys grouted with the same or similar non-shrink cement grouting mixes. Tests were conducted in the sequences mentioned before and numerical data were collected, in addition to a visual monitoring and video taping of structural changes in the key region. Three successful tests were completed for the top shear key location using non-shrink grout. Labels for these tests were TKSA1, TKSA2 and TKSA3. Failure in all these tests occurred as a bond failure between the shear key and the concrete surface of the key-way, mostly at the side of the central girder where tensile stresses were the greatest.

Failure occurred in the three tests at load level varied between 8 to 12 Kips (35.7 to 53.5 kN) with an approximate average failure load of 10 Kips (44.6 kN). This failure load is about equal to the design load, i.e. no factor of safety exists, nor would there be an expected fatigue life, since this failure took place after only one cycle of static loading. Figure 3.4. shows a picture of a typical cracked shear key after testing.

When testing the new proposed shear key design, located at the neutral axis, static loading could be carried out with no apparent cracks up to a load level as high as 26 Kips (116 kN). Three successful tests were completed for the middle shear key location using a non-shrink grout material. Labels for these tests were MKSA1, MKSA2 and MKSA3. Failure started at the bottom of the key as a small crack in the shear key itself and did not propagate significantly prior to reaching load level 30 Kips (134 kN), where tests were terminated. Figure 3.2. shows a picture of the proposed shear key modification during testing.

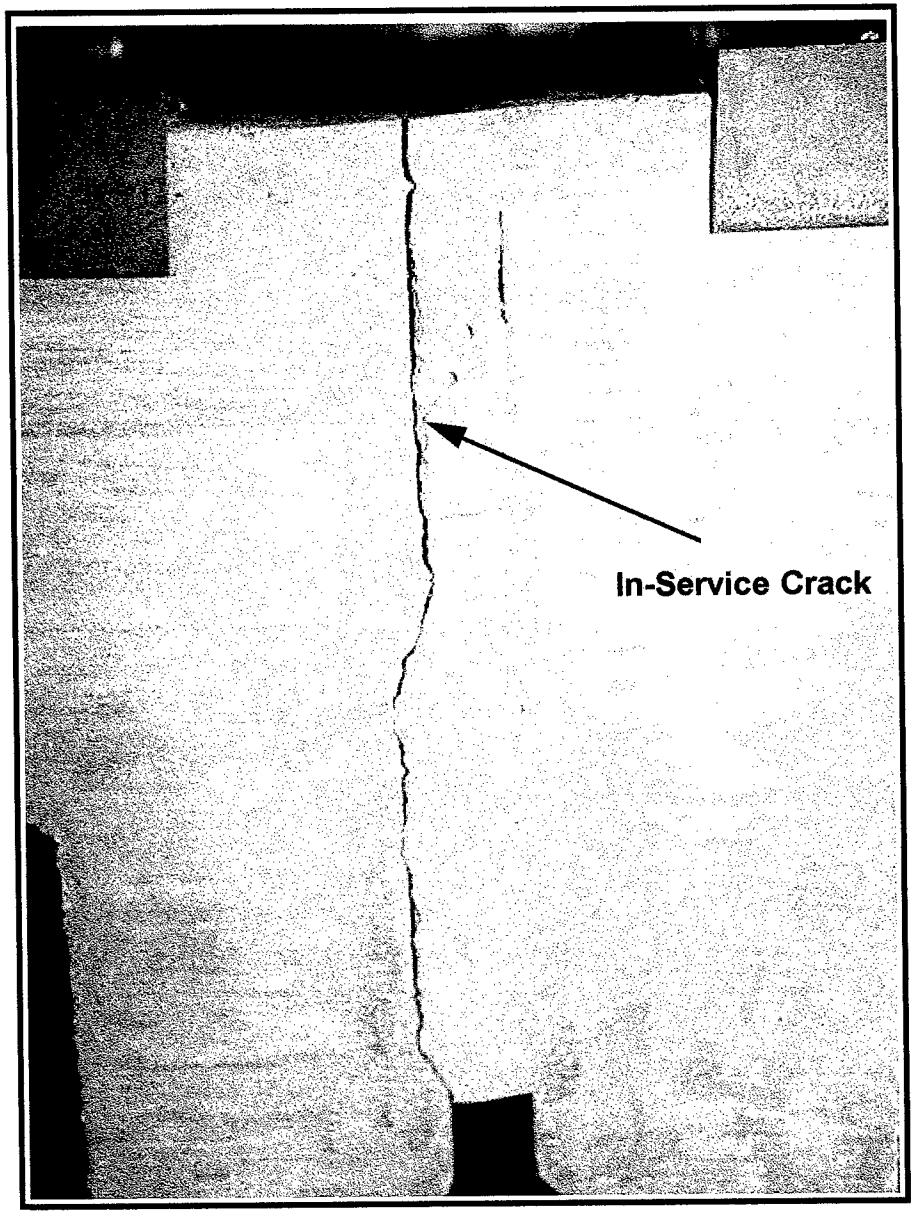

•Figure 3.1 Typical Shearkey Failure; Current Keyway Design

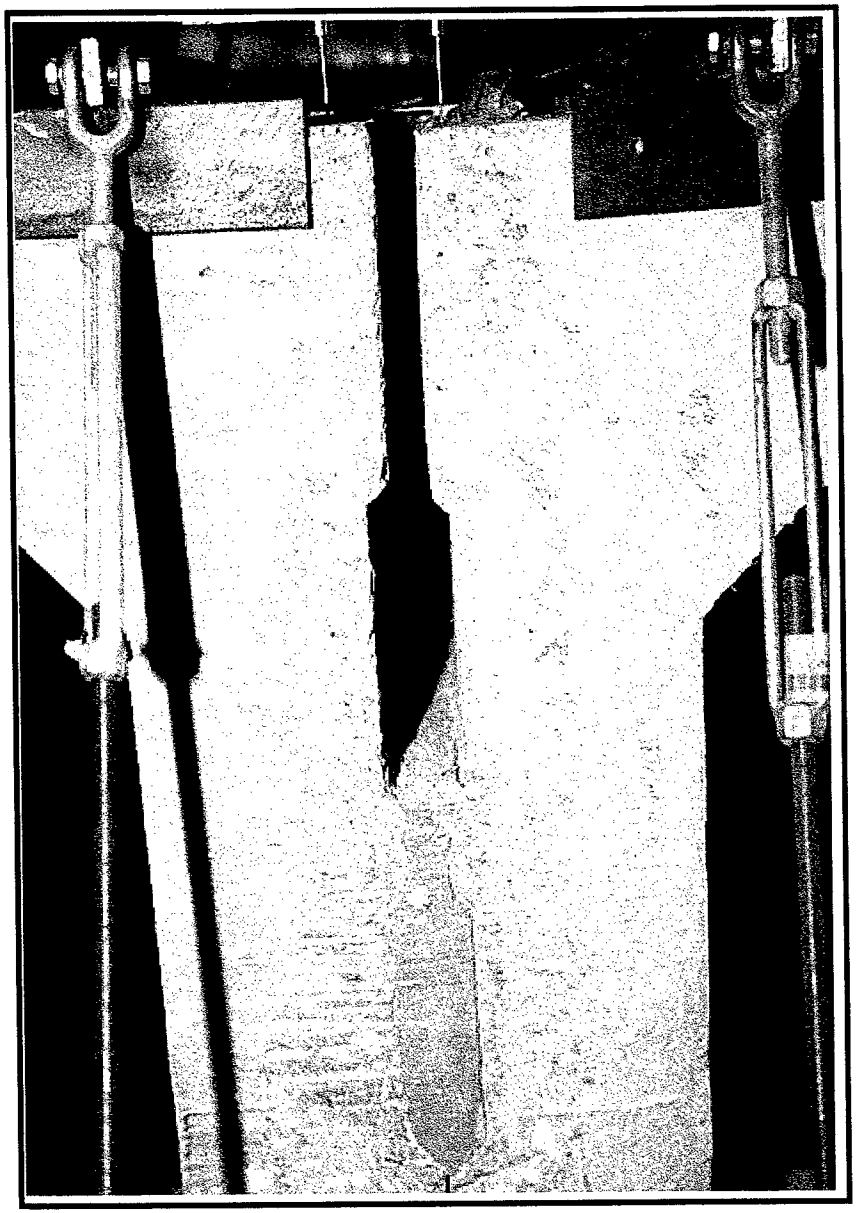

Figure 3.2 Test Specimen with Modified Keyway Design

The initial cracking load of the three tests were 24, 21 and 26 kips (107, 93.6 and 116kN) approximately, with an average of 23.5 Kips (105 kN). The average failure load as shown is approximately 2.3 times the average failure load for the current shear key design.

3.2.2. Mag-Phosphate Grout Shear Key Tests

This material, which is often used as a pavement repair material, due to its short setting time, has been marketed as a grout substitute. Using this material has been reported to result in a stronger key, with enhanced bond strength to concrete. When utilizing this material in the experimental program, however, difficulties were encountered with surface preparation. This material's major drawback is that it reacts very aggressively with any concrete surface containing almost any degree of carbonation. This reaction produces CO_2 gas which results in a porous layer at the interface between the concrete girder and the key. This porosity obviously minimize the overall contact area between the key and the girder, and generally weakens the bond between them. It was found throughout the experience of this investigation that it is very difficult to prevent any recarbonation of the concrete surface between surface preparation and placement of the grout. In an actual bridge project, with the time required between sand blasting the surfaces of 10, or more, 40 ft, or more, long girders on both sides, moving them, placing them, mixing and placing grout, it is difficult to see how recarbonation can be adequately prevented..

With the best precautions and protections available in the lab environment, three successful tests were completed out of four attempts. The four tests were labeled TKSB1, TKSB2, TKSB3 and TKSB4. The test results of only the three later specimens were considered valid. The failure load for these tests were approximately 12, 14 and 16 Kips (53.5, 62.4 and 71.3 kN) with an average of 14 Kips (62.4 kN). This means that the failure load level using this grouting material was approximately 40% greater than the failure load level when using the original non-shrink grout.

Figure 3.3 shows a close-up picture of the inner surface of the shear key after failure. It shows the size of the voids created by the trapped CO_2 gas, due to the chemical reactions with the

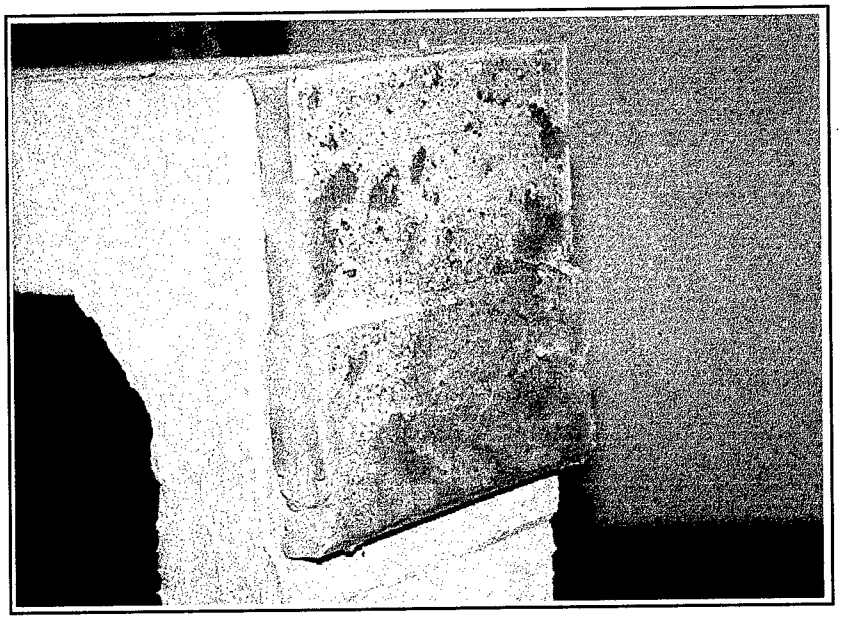

Figure 3.3 Failure Surface of Mag-Phosphate Grouted Keyway Following Testing

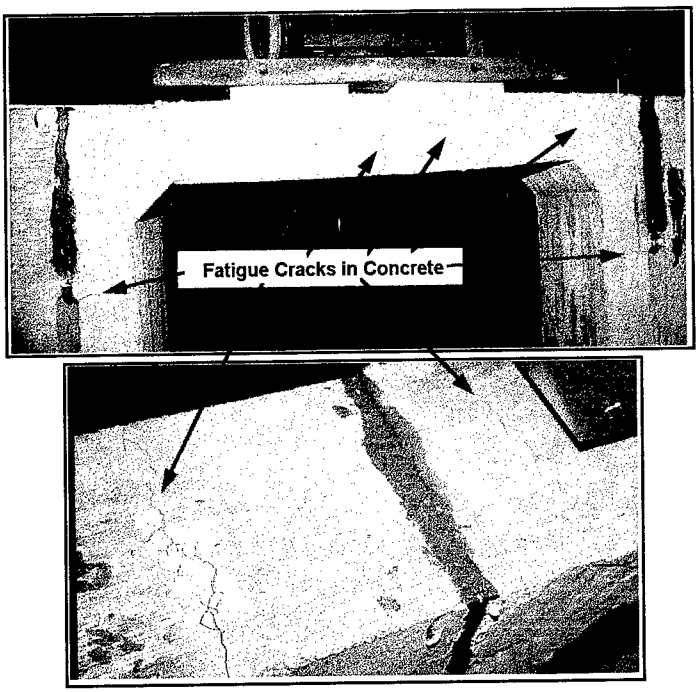

Figure 3.4 Current Keyway Design Specimens with Filled Epoxy Grout

recarbonated sections. Some of these surfaces, as mentioned in chapter 2, took about one hour per square foot of preparation in the lab, and some were taken to a commercial sand blaster to ensure good removal of the carbonated layer. All were grouted within a few hours of surface preparation, but some recarbonation had obviously taken place.

One can reasonably predict, from the test results for the modified key design using non-shrink grout material , discussed in 3.2.1., that a proportional result will be obtained if testing the modified key using mag-phosphate grout for the shear key. Results will be assumed to come somewhat higher than those indicated in 3.2.1, which would have exceeded the static load capacity of both the load fixture and the top flange of the specimen inself.

3.2.3. Epoxy Grout Shear Key Tests

This type of grout produced a shear key which did not fail within the capacity of the load fixture, even with the current shear key design. Epoxy was strong in both tensile strength and bonding strength with the concrete. Loading was carried out to load levels close to 40 Kips (178 kN) static loading, with no evidence of damage to the epoxy grouted shear keys. Static testing was terminated both due to concern for the capacity of the box cross sections themselves, and due to the usable capacity of the load fixture.

The epoxy grout shear key is considered, from a strength view point, a successful candidate as a structural solution. When looking at the safety of the individual girders in case of any unexpected over loading on the bridge, however, it is more favorable to have damage in the shear key, which possibly can be repaired, rather than having it in a major structure element, such as the girder itself. Figure 3.4 shows a photo of an epoxy shear key, where the epoxy exceeds the capacity of the concrete. Figure 3.5 pictures "dismantling" of an epoxy specimen, where the adjacent, concrete was damaged in the process, with no apparent distress in he epoxy grout.

Again, repeating these tests for the proposed middle key design was not necessary ,since it

Figure 3.5 "Dismantling" Epoxy Grouted Keyway Specimen

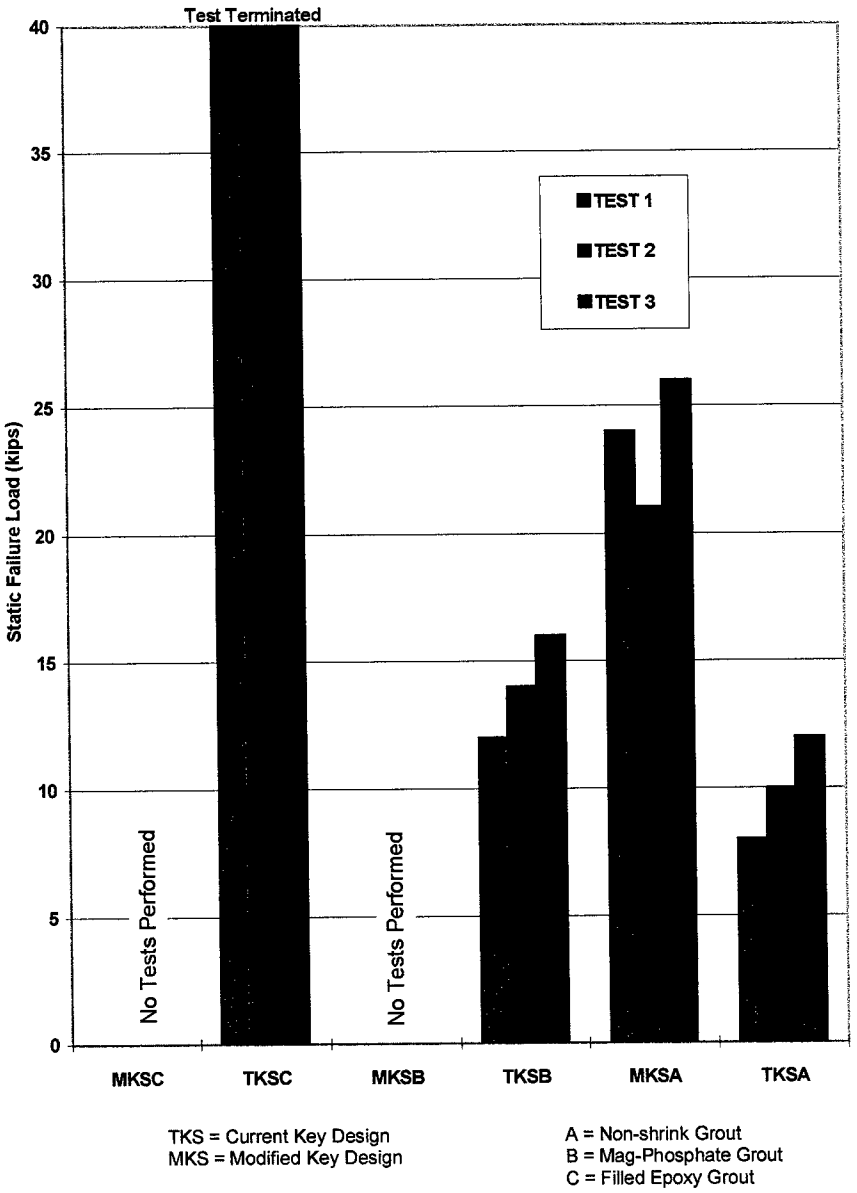

Figure 3.6 : Summary of Static Testing Results

can be expected, from 3.2.1, to survive well over 40 Kips of static loading, which was beyond the fixture capacity, as well as beyond the capacity of the box section flange for such loading. Results of static testing are summarized graphically in Figure 3.6.

3.3. Fatigue Tests Result

The main parameter of the fatigue test results were the number of cycles survived before a shear key failure took place. The same sequence of experimental program, as described for the static test group, was followed.

Figure 3.7 shows a log scale plot of the final results of all tests achieved. Two sets of tests were not performed; both the middle key tests using a mag-phosphate grouted shear key and an epoxy grouted shear key were omitted, as a result of knowing from the strength relation between these two materials and the ordinary non-shrink grout, that static failure would not have occurred within the load capacity of neither the fixture nor the specimen.

When non-shrink grout was tested in the top shear key fatigue test, the results came out as expected from the previously performed static loading tests. Three successful tests recorded less than one hundred cycles to failure. It is worth mentioning that in this case the number of cycles shown in figure 3.7 are not necessarily the actual number at failure. One hundred cycles in these tests took less than one minute which is about the time between finishing the start up of the test and initial observation of the shear keys. Failure could happened any where from one cycle up to the recorded cycle count. In most structure fatigue tests, one hundred cycles would be considered a negligible fatigue life.

Again as demonstrated in the static tests, using the alternative mag-phosphate grout in the top shear key only added about forty percent to the shear key capacity, as compared to non-shrink grout. One cannot expect a great increase in the life span of the shear keys under these conditions. Recorded results from the three successful tests are shown in Figure 3.7. The maximum lifetime

obtained was approximately one thousand cycles until failure.

Epoxy grouted shear keys were tested also for the sake of completeness. All tests were run until two million load cycles. Tests were then manually terminated. No failure, as expected, occurred in the shear key, nor in the bond with the concrete section. Cracks were prominent in the concrete box girder, adjacent to the keyway, however, due to the tensile stresses created by the continuity between the top flanges (see Figure 3.4). Tests for repeated cycling load for the shear key in the modified geometric design were limited to the non-shrink grout only. The first test exhibited a lifetime of 2,000,000 cycles to match the epoxy grout top key test, but with less extensive concrete cracking. This test was intentionally terminated at 2,000,000 cycles. The second test was run to 4,000,000 cycles to confirm the major difference between the two studied designs. The third test was run to 8,000,000 cycles which took more than one month of continuous running, until it was terminated without a failure. Figure 3.8. pictures the new non-shrink grout shear key after termination of a fatigue test. All three tests ended with the shear keys sound and intact, and completely bonded to the concrete sections. The concrete girders were less extensively cracked than in the top shear key tests.

Using mag-phosphate grout or epoxy grout could add no more to the expected lifetime of this design, which acquired its effectiveness from the advantageous location of the shear key, no matter what grouting material was used.

3.4. Additional Tests

3.4.1. Current Keyway Filled "Half way"

During the execution of the experimental program, a number of questions were raised for discussion. One of these question was, instead of moving the whole key to the neutral axis, would it be equally effective to terminate grouting six inches from the top, as shown in Figure 3.9, so as to interrupt the tensile stress progression through the top flange.

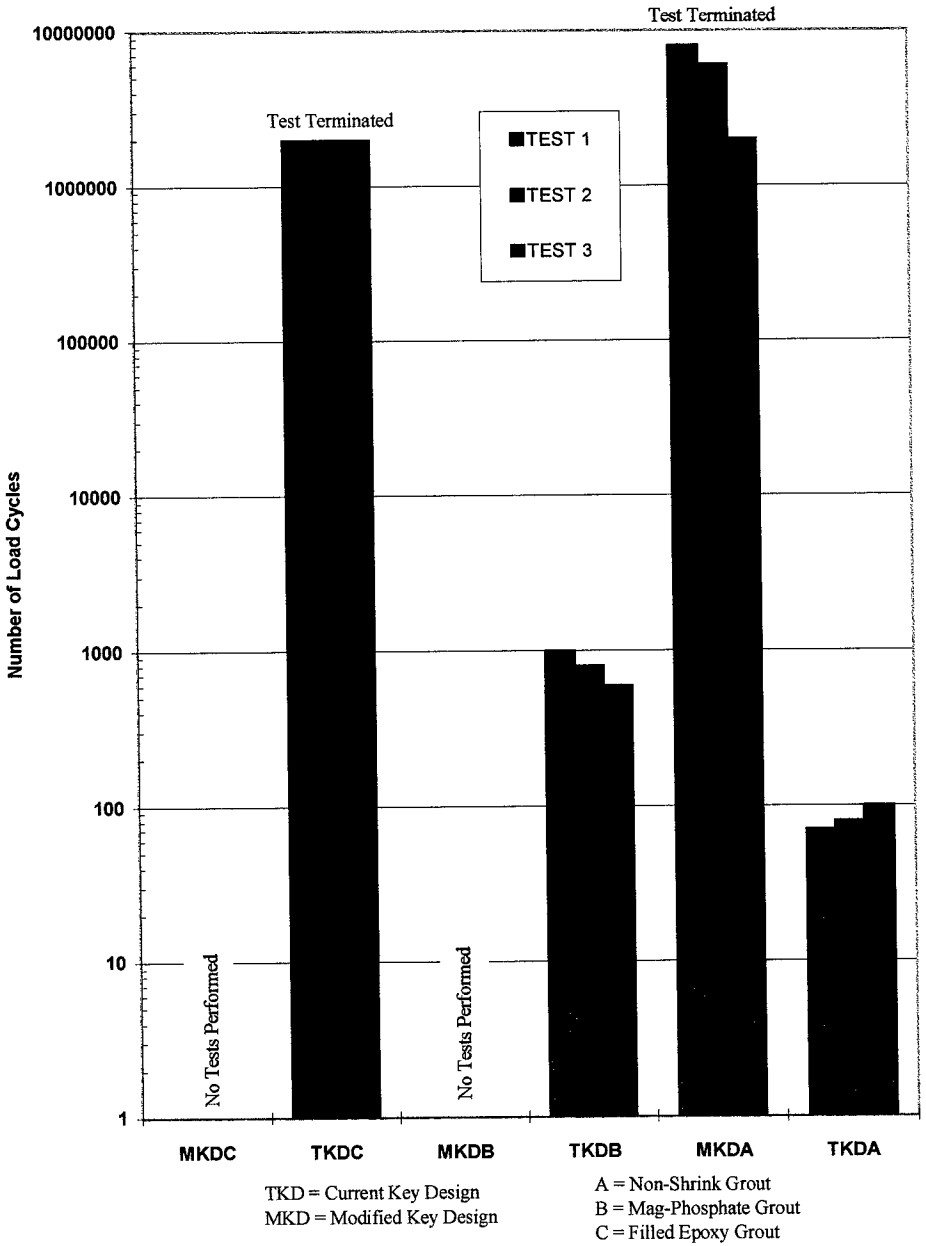

Figure 3.7: Summary of Results From Fatigue Testing

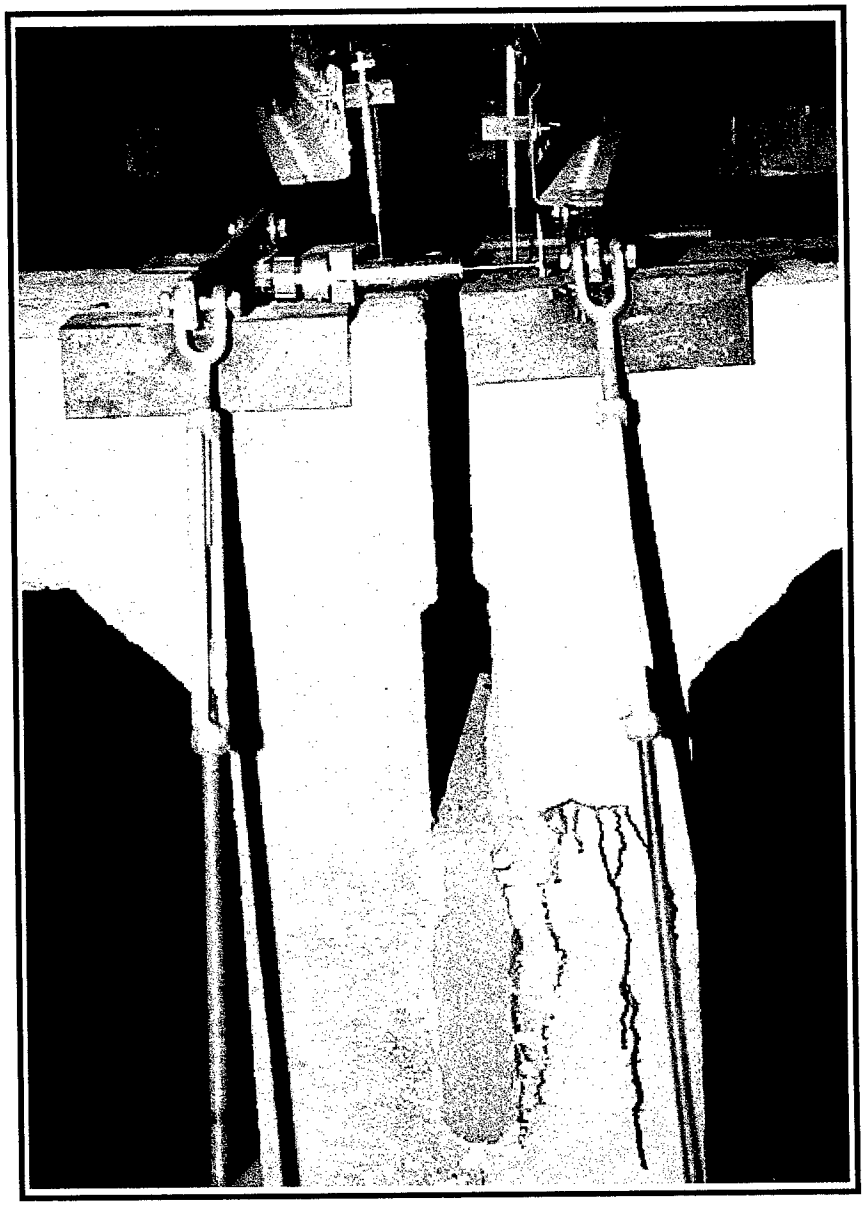

Figure 3.8 Modified Shear Key After 8,000,000 Load Cycles

To answer this question a 2D finite element analysis as well as a complete static loading test was carried out. The 2D analysis predicted tensile stresses in the topmost part of the shear key itself on the order of 750 psi (5.17MPa), which would create a likely initiation point for a crack. A typical three girder assembly test was conducted using the "half way" grouted shear key. The grouting material used was the mag-phosphate grout. All the prescribed setup and procedures for the previous tests were maintained.

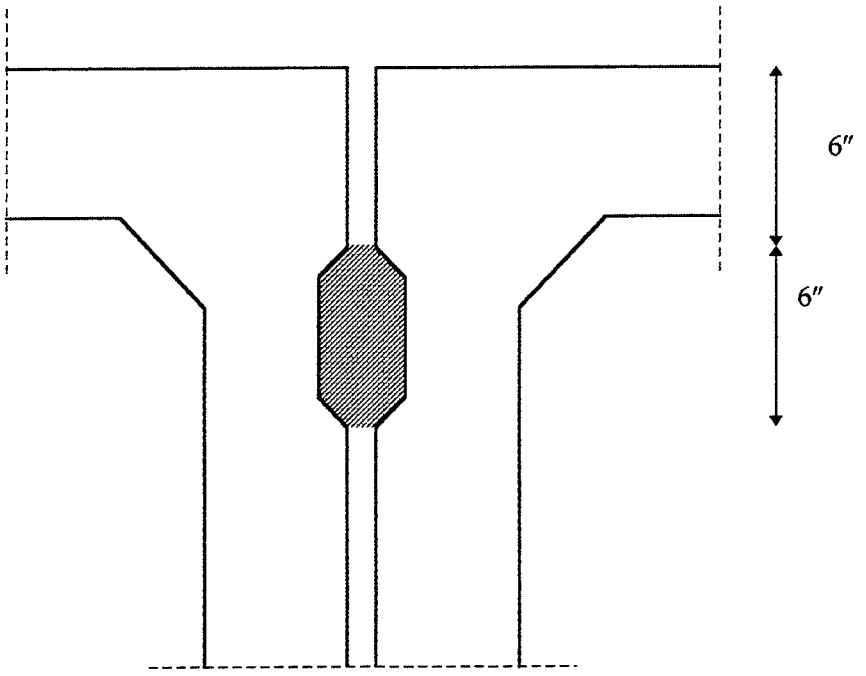

Fig. 3.9: Shear Key Grouted "Half Way"

When the static load approached the load level of 7.0 Kips (31.2 kN), a crack started through the shear key, initiating from the topmost portion of the grouted keyway. The location of the crack was very much in agreement with the implication of the 2D finite element analysis. As the load

increased the crack propagated smoothly , until it passd completely throught the grouted portion of the keyway.

3.4.2. Repeated Cycling Load of Lower Value

When the two dimension finite element model was implemented to analyze the problem and validate the test in its "slice" form, a full wheel load of 10 Kips (44.5 kN) was used in both the analysis and the fatigue tests. This decision was based upon observations from the preliminary three dimensional finite element analysis of a three girder subassemblage, which showed that the greatest portion of the lateral load transfer occurred within a short distance of the actual location where the wheel load was applied. Due to possible variations of the span, the depth and width of the girder, etc., load transfer may not be quite as concentrated, hoever, in some instances. From a limited FE parameter study, in which the top flange was modeled as a plate supported on two edges, a 4 Kip (17.8 kN) load was also considered in testing the 2D specimens, as a lower bound load transfer requirement, for the full 10 Kips design wheel load.

Reviewing the results of all the experimental tests presented earlier in this chapter it is obvious that using the larger equivalent load will be in the conservative side. All of the tests which survived over million of cycles in fatigue would clearly survive longer using a lower load under the same conditions. The only two tests for which the results could be significantly affected is the top key tests, using both non-shrink grout and mag-phosphate grout. Reducing the cyclic load in these two tests might increase their life span before failure. To determine the magnitude of this possible increase, a typical TKDB test was repeated using a load of 4.0 Kips (17.8 kN) instead of 10.0 Kips (44.6 kN). This test recorded 1300 cycles before failure. Although the increase is about 30% of the previous recorded mag-phosphate grout result, it is still far from an acceptable result. The outcome of this test was a confirmation that conclusions obtained from the original experimental program would not be significantly affected by changing the test load to a lower value.

CHAPTER FOUR: TESTS WITH AN OVERLAY IN PLACE

4.1 Specimen Description

As a follow-up to the initial test program, a limited series of fatigue tests were performed, utilizing test specimens essentially identical to those of the original program, but with a waterproofing membrane and asphalt concrete wearing surface overlay applied (see Figure 4.1 for typical details of a modified shear key specimen).

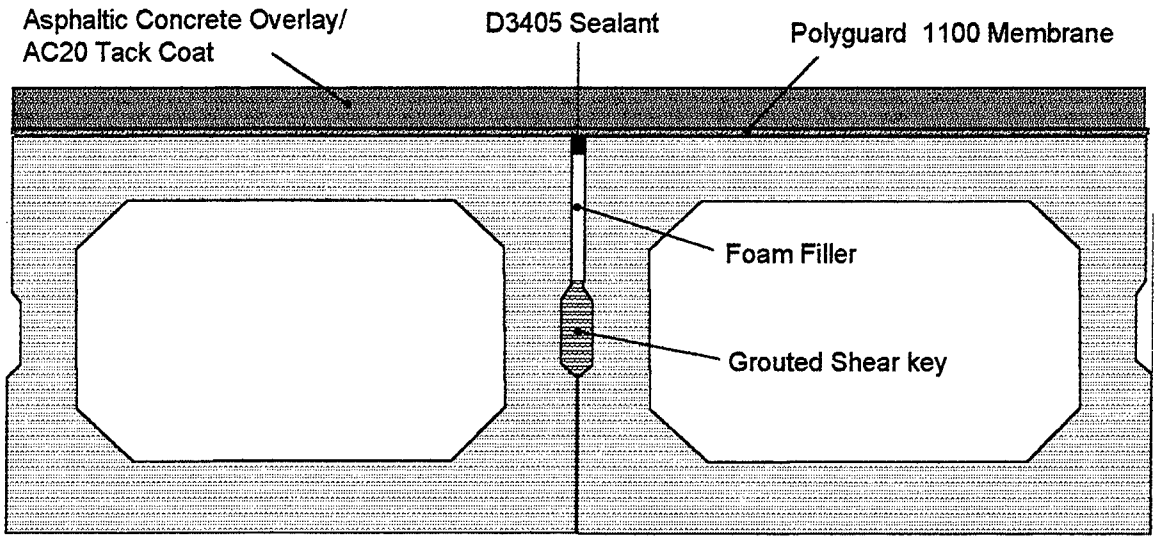

Figure 4.1 : Proposed Modified Shear Key Detail

4.2 Membrane and Overlay

The waterproofing membrane was applied according to provisions contained in ODOT proposal note 846-91, dated November 10,1994, which describes a "Sheet Type 3 Waterproofing Membrane", consisting of "a high density asphalt mastic sandwiched between two layers of polymeric fabric". Those provisions are summarized in the following two pages.

Summary of ODOT Proposal Note 846-91

Materials:

Primer/Sealant	ASTM D3405, ASTM D1190 or as recommended by membrane manufacturer
Membrane	PavePrep manufactured by the PavePrep Corp. OR Pro-Guard manufactured by Phillips Fibers Corp. OR Polyguard 1100 manufactured by Polyguard Products, Inc. OR Other products manufactured specifically for waterproofing bridge decks and meeting the following properties:

Physical properties of Membrane:

Thickness	3.43.mm (0.135 inches) min.
Width	.914 meter (36 inches) min.
Weight	3.875 kg/m^2 (0.8 lb/ft^2) min.
Tensile Strength	4.91 kg/mm (275 lbs/in) ASTM D 882 Mod.*
Machine Direction	1.4 kg/mm^2 (2000 lbs/in^2)
X-Machine Direction	2.677 kg/mm (150 lbs/in) ASTM D882 Mod.* 0.703 kg/mm^2 (1000 lbs/in^2)
Elongation @ Break	100% ASTM D 882 Mod.
Brittleness	Pass ASTM D517
Softening Point (Mastic)	93 deg. C (200 deg. F) min. ASTM D2398
Peel Adhesion	0.0357 kg/mm (22.0 lbs/in) ASTM D413*
Cold Flex 50mm x 125mm (2" x 5") Specimen	No Cracking ASTM D 146 180 deg. bend on 50mm (2") mandrel @ 18 deg. C (0 deg. F)
Heat Stability 50mm x 125mm (2" x 5") Specimen	No Dripping or Delamination Hung Vertically in a Mechanical Convection Oven 2 hrs @ 88 deg. C (190 deg. F)

* 300 mm (12 inches)/ minute test speed and 25 mm (1 inch) initial distance between grips

Surface Preparation:

Prior to placing the membrane, the surface to be waterproofed shall be clean, dry and free of protrusions. All dirt and dust shall be swept off and the surface air-blown clean. All joints or cracks greater than 10 mm (3/8 in) wide shall be filled with portland cement mortar and allowed to cure. Any oil or grease deposits shall be removed using water and a detergent designed for removing oil deposits from concrete surfaces together with power or broom scrubbing. The residue and detergent shall be thoroughly flushed from the surface. Traffic shall not be permitted on the cleaned surface prior to application of the primer/sealant and the membrane.

In some cases (if specified by plan note) it may be necessary to apply the membrane to a freshly milled or recently placed asphalt concrete surface. In either case, the surface to be covered shall be clean and free of loose material.

Application Procedure:

The surfaces to be waterproofed shall be dry and free of dust and loose particles and the ambient surface and material temperatures shall not be less than 4C (40F) during application. The structure shall be waterproofed from the low to the high side. On bridges with curbs, the primer and the membrane shall be placed 75 mm (3 in.) up the curb face.

A uniform coating of primer shall be applied at a rate of 2.2635 l / m^2 (0.5 gallon / yd^2). Primer shall be applied over a small over a small area of surface no further than 1.5m (5 ft.) in front of the membrane. An extra band of sealant shall be applied at the edge of the membrane to develop seal. membrane shall be overlapped 75 mm (3 in.) when putting down an adjoining roll. Primer shall be on top of adjoining roll and under lap. After entire surface is covered, all exposed lap edges shall be sealed with primer and smoothed with a V squeegee.

On prestressd box beam bridges that have no approach slabs, membrane shall extend over and down the end of beams to 150 mm (6 in.) below bridge seat. On prestressed box beams that have approach slabs, membrane shall extend out onto the approach slab 0.6 m (2 ft.) minimum.

Traffic may be allowed to operate directly on the completed membrane, with the Engineer's approval. If approved, any damage that occurs to the membrane before the asphalt concrete overlay is placed shall be repaired at the Contractor's expense.

Primer Heating:

An oil primer heated double-jacketed kettle shall be used for heating the primer. The kettle shall be essentially clean and free from other materials. While it is not necessary that the kettle be cleaned down to bare metal, any obvious build-up should be scraped out. A single jacket kettle may be used if using a primer which has the capability of being melted and heated to application temperatures in direct fire or heated single walled melting kettles and staying within the limit of the manufacturer's recommendation.

Sealant shall be heated to a temperature between the recommended pour temperature of 193C (380F) and the maximum safe heating temperature of 210C (410F). Top of membrane shall be conventionally tacked prior to overlaying with asphalt concrete.

4.3 Placement of the Membrane / Asphalt Concrete Overlay

Placement of the membrane / overlay consisted of a cleaning the surface of the beam sections, laying a tack coat of AC-20, placing a sheet type membrane layer (Polyguard 1100), followed by a tack coat of AC-20 and the ready-mix asphalt concrete overlay, typically placed in two lifts.

Conventional roller compaction of the asphalt concrete overlay was not possible for the 12 in. (0.3 m) thick 2-D "slice" beam sections. An alternative compaction scheme was developed employing the same 50 kip (223 kN) MTS actuator which was utilized for static and dynamic testing of the previous nonoverlaid specimens. A W12x 53 wide-flange beam was used as a dynamic "ram" for compacting the asphalt concrete layer between confining steel side forms (see Figure 4.2 and 4.3). The compacting pressure, generated by loading the W12x 53 ram with the MTS actuator, was first applied in sinusoidal fashion, with an amplitude of 2 psi (13.8 kPA) and a frequency of 3 hz for a period of approximately 30 minutes, followed by a static pressure of 30 psi (207 kPa) applied for a period of several hours, to allow final consolidation (see Figure 4.4).

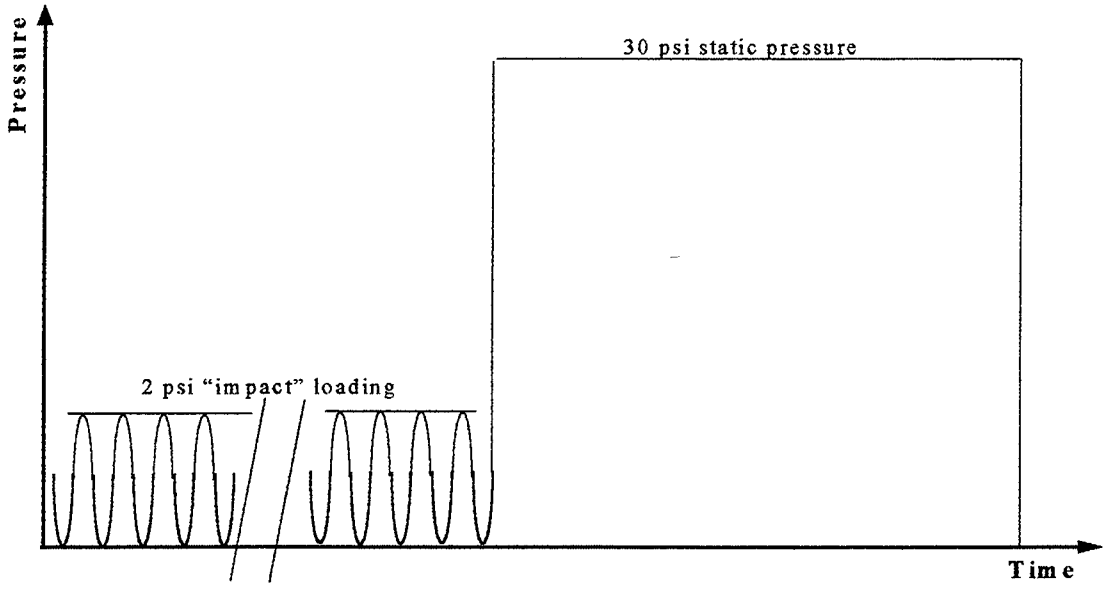

Figure 4.4 Compaction Pressure History

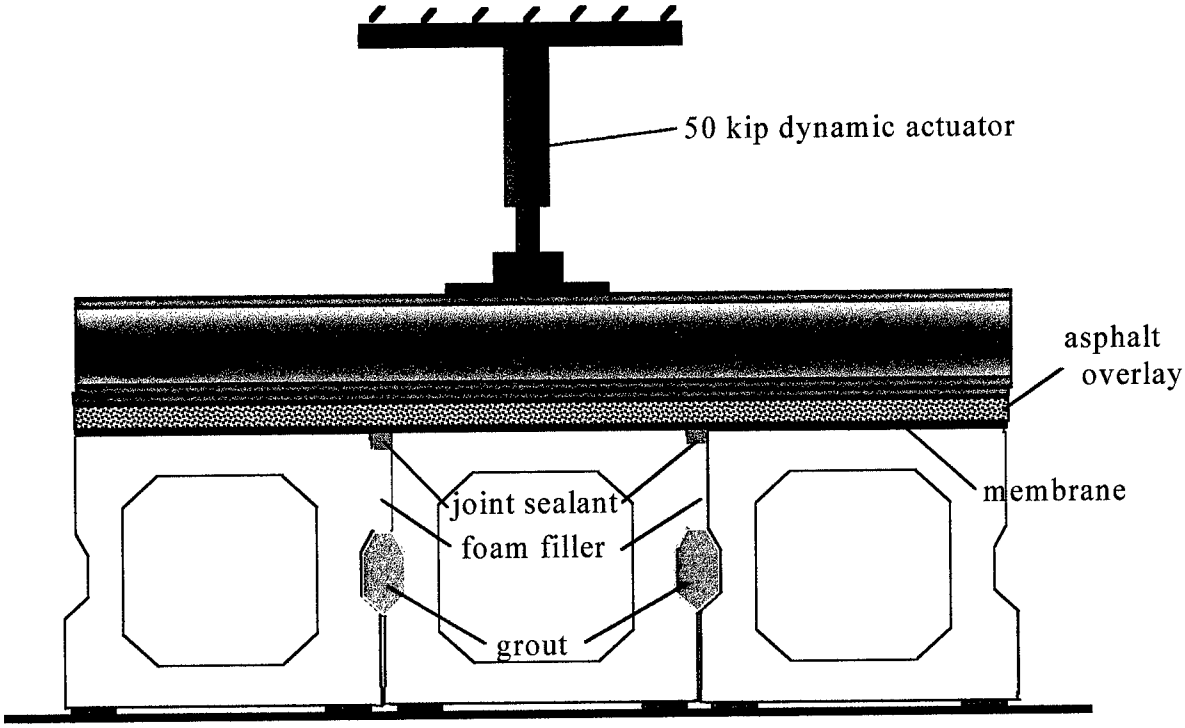

Figure 4.2 Overlay Compaction Scheme

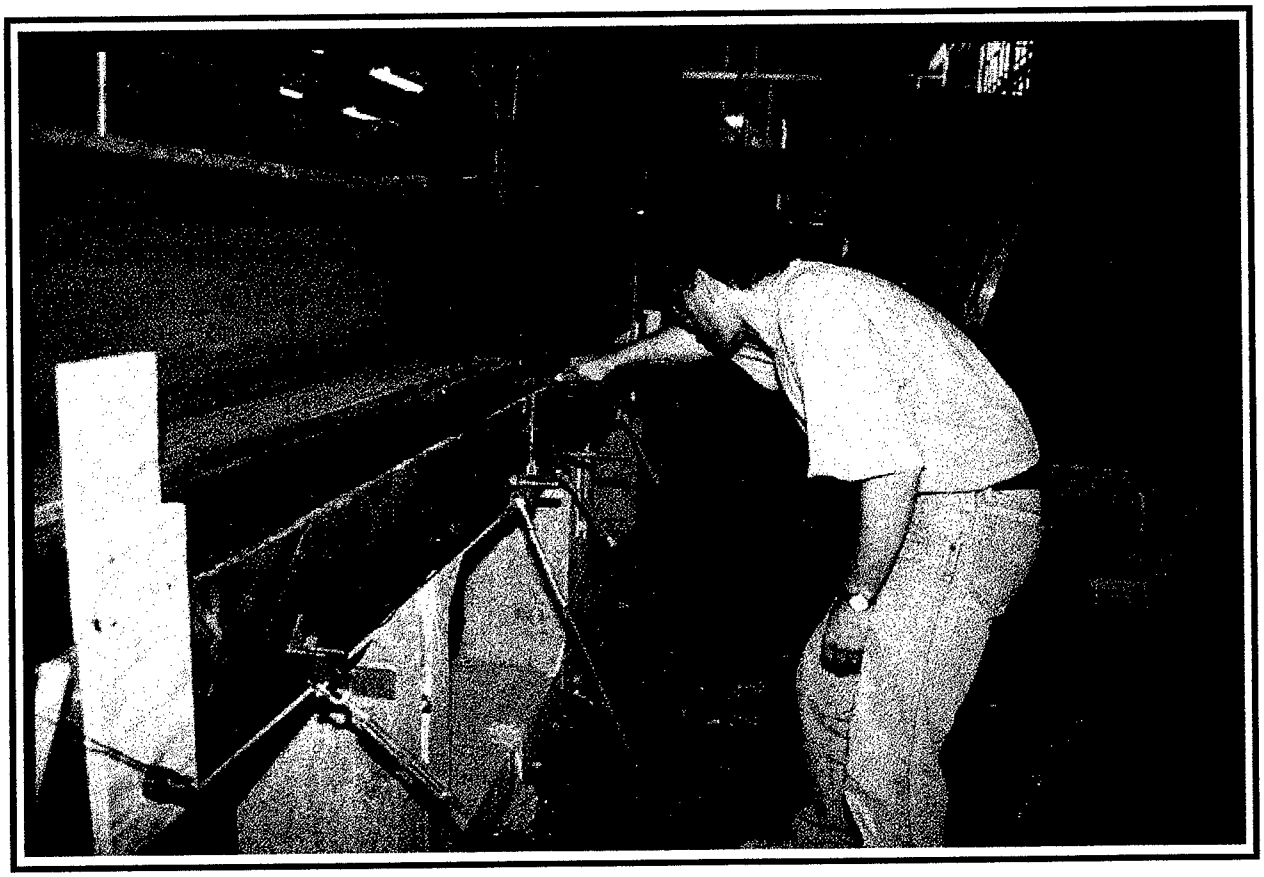

Figure 4.3 Overlay Compaction in Progress

4.4 Tests Conducted

Series of fatigue tests with were conducted on specimens grouted by the current shear key design, and by the modified shear key design, located at the neutral axis (see Figures 4.5&4.6). Cyclic loads of 10 kips (44.6 kN), similar to the loading utilized for the fatigue tests without an overlay, were applied. Watertightness of the membrane was periodically checked during the fatigue testing.

4.5 Results of Testing with a Membrane / Overlay in Place

Tests with the current shear key design universally experienced debonding of the shear key with a negligible number of load cycles, just as had been the case without an overlay (see Figure 4.5) . It was found, however, that watertightness of the Type III membrane was apparently maintained for a large number of load cycles, despite the debonding failures of the shear key. It is important to note, however, that the fatigue testing was conducted at laboratory room temperature (between 70 and 80 degrees Fahrenheit), and that the membrane and sealant materials remained extremely pliant throughout the tests.

Tests with the modified shear key location at the neutral axis also behaved just as they had in the tests without an overlay, i.e., no shear key failures were observed through a very large number of cycles. Eventually sufficient creep of the asphalt concrete occurred under the concentrated load points that testing was terminated, after approximately 1,000,000 cycles, with no signs of distress in any of the modified shear keys. As with the tests without overlays, the membranes all appeared to retain their watertightness throughout the testing, which was conducted at room temperature.

The apparent durability of the Type III membrane, with both of the shear key designs tested, may be in large part attributable to the room temperature test conditions. It would certainly be premature to draw definitive conclusions concerning low temperature durability based upon the limited room temperature test series conducted.

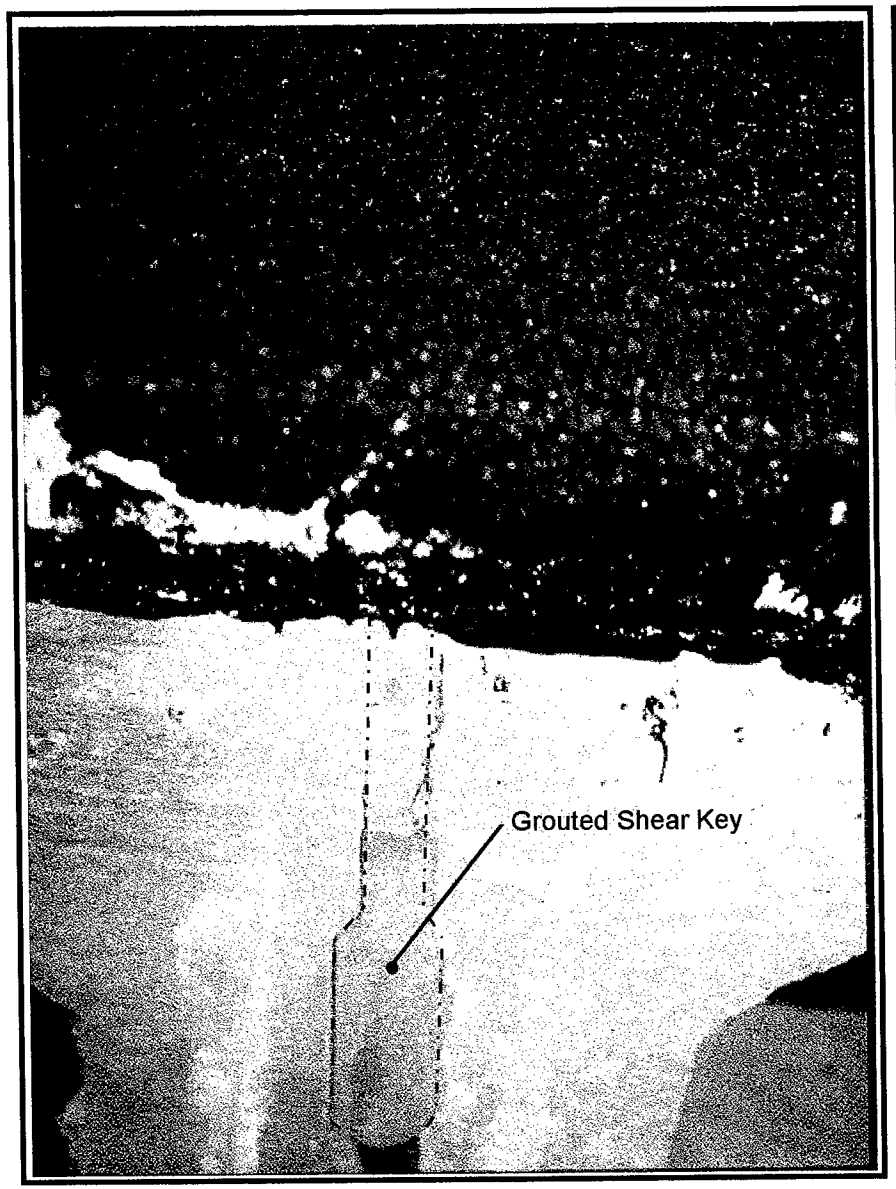

Figure 4.5 : Conventional Shear Key with Overlay

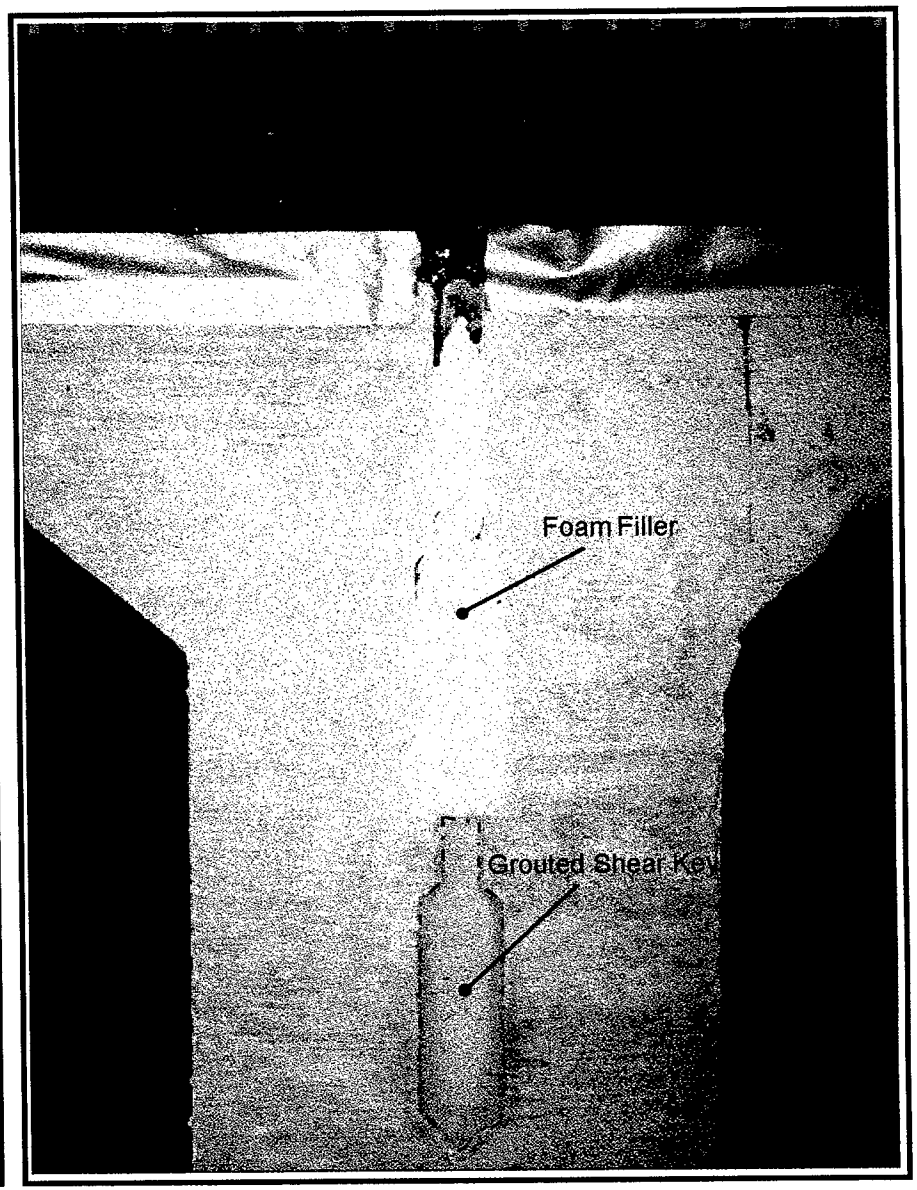

Figure 4.6: Modified Shear Key with Overlay

CHAPTER FIVE: CONCLUSION

5.1 Conclusions

Figure 3.6 summarizes the results of the completed static loading tests. Along with Figure 3.7, which summarizes the results of fatigue tests, it illustrates that the proposed shear key in the neutral axis location proved to be a viable candidate as an alternative shear key design.

Conclusions from field and laboratory tests throughout the study can be summarized by the following points:

1) There is a shear key failure problem as indicated from the observed leaking joints and confirmed by the relatively large differential displacement of adjacent box girders observed during field tests of prestressed box girder bridges.

2) Relative displacement between girders, occurring in a cyclic fashion, produces reflective cracking in the deck membrane and overlay. The reflective cracking leads to the ingress of waterborne deicing chlorides and substantial corrosion problems.

3) Severe corrosion, particularly of the prestressing strands adjacent to the leaking joints, can lead to structural damage and concern for the integrity of the bridge.

4) Finite element analysis clarified that the tensile stress arising from the negative transverse moment in the top flange of the bridge, generated due to the continuity provided by the shear key in the current location, may be responsible of the shear key failure.

5) A proposed new location for the shear key, at the neutral axis, performed well during both static and fatigue tests. Static load capacity was almost tripled from the current shear key design with the same grouting material. Fatigue life of the new shear key design was extended to over 8,000,000 cycles. Use of grouting material stronger than non-shrink grout was not required for the modified keyway design.

6) Mag-phosphate grouting material is very sensitive to carbonated concrete surfaces. It is difficult to provide a carbonate free concrete surface in the key ways to prevent the chemical reaction with mag-phosphate grout. The fast setting times for mag-phosphate grout would offer advantages in construction, particularly for bridge replacements.

7) Epoxy grout is a very strong grouting material, which also exhibits excellent adhesion to concrete. In addition to greater difficulties in preparing the grout, with the needed accuracy in proportioning and mixing the resin, hardener and filler, long term epoxy grout behavior under temperature cycles is perhaps questionable, with little long term field experience currently available.

8) The newer Ohio "Sheet Type 3" membranes tested are very tolerant , at least at laboratory room temperatures, of relative displacements within the shear keys. The leaking joints observed in the earlier field studies were all on bridges constructed with older membrane specifications, which had been in service for a number of years (typically 15 years or more), over a wide range of environmental conditions.

5.2 Implications of the Study

The structural effectiveness of prestressed precast concrete box girder shear keys can be enhanced by using the conventional non-shrink grout with the new shear key design. Eliminating shear key failure problems should help mitigate corrosion problems from leaking joints. More expensive materials, such as mag-phosphate or filled epoxy grouts, may not be needed for the shear key, if the drawbacks in current structural performance can be avoided. Routine repair requirements for shear keys should be minimized.

5.3. Suggestions for future work

1) Additional research to investigate modifications of the geometric shape and dimensions of the shear key would be desirable.

2) Investigation of the performance of membrane materials, when subjected to realistic relative movements at intergirder joints, is needed over the full range of temperature/chemical conditions encountered in actual bridges in Ohio. Even in the modified shear key design, where the larger (observed in the field to be as high as 20 mils (.5 mm)) "shearing" deformations exhibited at the shear keys are eliminated, smaller horizontal "opening and closing" deformations still occur across the joint with load cycles, which the membrane must withstand. Measurements made of these horizontal displacements during the laboratory testing (see the horizontal displacement transducer in Figure 3.8) indicated a peak-to-peak amplitude of approximately 8 mils (.2 mm) for a 10 kip (44.5 kN) cyclic load on the 2-D "slice" specimens. The limited testing performed at room temperature is not an adequate test of the in-situ performance to be expected.

REFERENCES

1. *1995 Annual Book of ASTM Standards, Designations: C 93 - 90, C 109 - 92, C 307 - 83, C 496 - 90 and C 1107 - 90*, American Socity for Testing and Materials, Philadilphia, PA. 1995.

2. *AASHTO Standard Specifications of Highway Bridges*, Fifteenth Edition, American Association of State Highway and Transportation Officials, Washington D.C. 1992.

3. ACI Committee 503, "Use of Epoxy Compounds with Concrete", *ACI 503R-89*, American Concrete Institute, 1989

4. Annamalai, G. and Brown, R.C., "Shear Transfer Behavior of Post-Tensioned Grouted Shear-Key Connections in Precast Concrete-Framed Structures", 1990. *ACI Structural Journal*, 87.1:53-59.

5. Bakht, B., L.G. Jager and M.S. Cheung. 1983. "Transverse Shear in Multibeam Bridges." Proc. *ASCE, Journal of the Structural Division*. 109.4:936-949.

6. Bender, Brice F., and Kriesel, William G., "Precast, Prestressed Box Beams; A state-of-the-art Report," *PCI JOURNAL*, V.14, No. 1, February 1969. pp. 72-95.

7. *Bridge Bulletin*, Precast/Prestressed Concrete Institute, Chicago, IL, Winter 1990.

8. Cheung, M.S., B. Bakht and L.G. Jaeger. 1982. "Analysis of Box Girder by Grillage and Orthotropic Plate Methods." *Canadian Journal of Civil Engineering*. 9.4:595-601.

9. Connecticut Department of Transportation, 1992. *Design Standards for Prestressed Box Girders*. Hartford, Conn.

10. Fereig, S., "Preliminary Design of Precast Prestressed Concrete Box Girder Bridges", *PCI JOURNAL*, May/June 1994. pp. 82-90.

11. Huckelbridge, A. A., El-Esnawi, H., and Moses, F. " An Investigation of Load Transfer in Multi-Beam Prestressed Box Girders," *Final Report*, Ohio Department of Transportation/ FHWA, Columbus, Ohio.

12. Huckelbridge, A. A., El-Esnawi, H., and Moses, F. "Shear Key Performance in Multibeam Box Girder Bridges", *ASCE Journal of Performance of Constructed Facilities*, Vol. 9, No. 4, Nov. 1995, pp. 271-285.

13. Jaeger, L.G. and Bakht, B. "The Grillage Analogy in Bridge Analysis." *Canadian Journal of Civil Engineering*. 0:224-235, 1982.

14. Kaneko, Y., Connor, J.J., Triantafillou, T.C., Leung, C.K., "Fracture Mechanics Approach for Failure of Concrete Shear Key. I: Theory", *ASCE, Journal of Engineering Mechanics*. 119.4:681-699, 1993.

15. Kaneko, Y., Connor, J.J., Triantafillou, T.C., Leung, C.K., "Fracture Mechanics Approach for Failure of Concrete Shear Key. II: Verification", *ASCE, Journal of Engineering Mechanics*. 119.4:701-719, 1993..

16. Mikkola, M.J. and J. Raavola. "Finite Element Analysis of Box Girders." *ASCE, Journal of Structure Division*. 106:1343-1357, 1980.

17. Sanders, W.W. and H.A. Elleby. "Distribution of Wheel Loads on Highway Bridges." *NCHRP Report 83*: p.56, 1970.

18. Shushkewich, K. W. "Approximate Analysis of Concrete Box Girder Bridges." *ASCE Journal of Structural Engineering*. 114.7:1644-1657, 1988.

19. Stanton, J.F. and Mattock, A.H. "Load Distribution and Connection Design for Precast Stemmed Multi-Beam Bridge Superstructures" *NCHRP Report 287*, Transportation Research Board, Washington, D.C., 1986.

20. Wilson, E.L., and Habibullah, A., "SAP90, Program User's Manual"" Computer & Structures, Inc. 1990.

21. Young, D. and Huckelbridge, A.A., "Effect of Relative Flexural/Torsional Characteristics Upon Load Distribution in Multi-Beam Prestressed Concrete Bridges", *Final Report: Ohio Department of Transportation /FHWA*, Columbus, Ohio, 1993.

22. Ziverts, George J., "A Study of Cardboard Voids for prestressed Concrete Box Slabs," *PCI JOURNAL*, V. 9, No. 3, June, 1964, pp. 66-93 (part I) and No. 4, August 1964, pp. 33-60 (parts II, III and IV).

23. Zokaie, T., Osterkamp, T.A., Lmbsen, R.A., 1991. "Distribution of Wheel Loads on Highway Bridges, "Final Report, *NCHRP 12-26*, Transportation Research Board, Washington D.C.

24. Zollman, Charles C., "Dynamic American engineers sustain Magnel's momentum," *PCI JOURNAL*, V. ?, No. ?, July-August 1978, pp. 30-63.